iScience

CellPress

Article

α-Synuclein Translocates to the Nucleus to Activate Retinoic-Acid-Dependent Gene Transcription

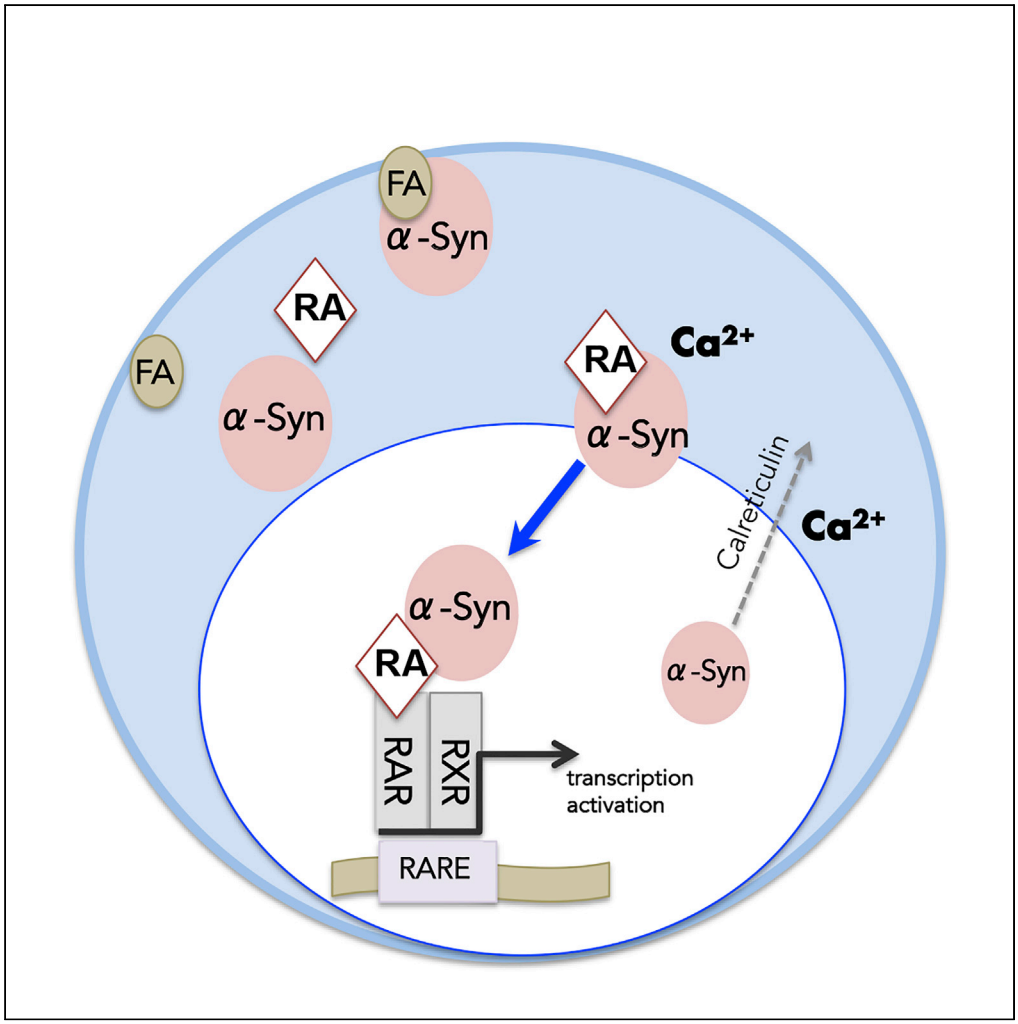

Dana Davidi, Meir Schechter, Suaad Abd Elhadi, Adar Matatov, Lubov Nathanson, Ronit Sharon

ronitsh@ekmd.huji.ac.il

HIGHLIGHTS

α-Syn normally binds RA and translocates to the nucleus to regulate transcription

Nuclear translocation of α-Syn is regulated by calreticulin and Ca^{2+}

Nuclear translocation of α-Syn is linked to PD

Davidi et al., iScience *23*, 100910
March 27, 2020
https://doi.org/10.1016/j.isci.2020.100910

iScience

CellPress

Article

α-Synuclein Translocates to the Nucleus to Activate Retinoic-Acid-Dependent Gene Transcription

Dana Davidi,[1] Meir Schechter,[1] Suaad Abd Elhadi,[1] Adar Matatov,[1] Lubov Nathanson,[2] and Ronit Sharon[1,3,*]

SUMMARY

α-Synuclein (α-Syn) protein is implicated in the pathogenesis of Parkinson disease (PD). It is primarily cytosolic and interacts with cell membranes. α-Syn also occurs in the nucleus. Here we investigated the mechanisms involved in nuclear translocation of α-Syn. We analyzed alterations in gene expression following induced α-Syn expression in SH-SY5Y cells. Analysis of upstream regulators pointed at alterations in transcription activity of retinoic acid receptors (RARs) and additional nuclear receptors. We show that α-Syn binds RA and translocates to the nucleus to selectively enhance gene transcription. Nuclear translocation of α-Syn is regulated by calreticulin and is leptomycin-B independent. Importantly, nuclear translocation of α-Syn following RA treatment enhances its toxicity in cultured neurons and the expression levels of PD-associated genes, including ATPase cation transporting 13A2 (ATP13A2) and PTEN-induced kinase1 (PINK1). The results link a physiological role for α-Syn in the regulation of RA-mediated gene transcription and its toxicity in the synucleinopathies.

INTRODUCTION

α-Synuclein (α-Syn) protein critically associates with the onset and progression of Parkinson disease (PD). It is a major constituent of Lewy pathology, the hallmark pathology of PD and additional neurodegenerations, classified as synucleinopathies. Its toxicity involves multiple cellular organelles including, synaptic vesicles, mitochondria, ER and Golgi, lysosomes and autophagosomes, and the nucleus (reviewed in (Wongand Krainc, 2017)).

Previous studies suggested physiological roles for α-Syn in regulating membrane lipid content and curvature (Varkey et al., 2010); SNARE complex assembly (Burre et al., 2010); clathrin-mediated endocytosis (Ben Gedalya et al., 2009); and dopamine metabolism (Al-Wandi et al., 2010). Nevertheless, the mechanism of α-Syn action in these divergent cellular functions is only poorly understood.

Nuclear localization of α-Syn was first described in neurons innervating the electric organ of the Torpedo, a marine elasmobranch species (Maroteaux et al., 1988). Yet, due to difficulty to experimentally direct α-Syn to the nucleus, the biological significance of nuclear α-Syn has been debated for a long time. Growing evidence now suggests that nuclear α-Syn associates with its toxicity in neurodegeneration. TRIM28, a protein involved in transcription and DNA repair, was shown to regulate α-Syn toxicity and accumulation in the nucleus (Rousseaux et al., 2016). Additional studies reported the involvement of α-Syn in DNA damage however, with conflicting results (Milanese et al., 2018; Paiva et al., 2017; Schaser et al., 2019; Vasquez et al., 2017). Targeting α-Syn to the nucleus, by constructing a nuclear localization sequence (NLS) upstream of its open reading frame, enhanced its toxicity in a fly model for synucleinopathy (Kontopoulos et al., 2006). The PD-causing mutations A30P, A53T, and G51D in α-Syn were shown to increase its nuclear accumulation (Fares et al., 2014; Kontopoulos et al., 2006). It has been suggested that nuclear α-Syn is involved in transcription regulation, including downregulation of Nurr1, a nuclear receptor that is essential for the development and specification of midbrain dopamine neurons (Decressac et al., 2012), and PGC-1α, a transcriptional regulator involved in metabolism of energy and mitochondrial homeostasis (Eschbach et al., 2015; Zheng et al., 2010). α-Syn's effects in transcription regulation are potentially mediated through its binding to DNA (Pinho et al., 2019), histones (Goers et al., 2003; Liu et al., 2011), and chromatin (Vasquez et al., 2017).

The vitamin-A metabolite, retinoic acid (RA), plays key roles in embryonic development and in tissue remodeling in the adult organism (Canete et al., 2017). Most of the cellular effects of RA are attributed to its regulation of transcription, controlled mainly by three retinoic acid receptors (RAR) α, β, and γ,

[1]Biochemistry and Molecular Biology, IMRIC, The Hebrew University-Hadassah Medical School, Ein Kerem, 9112001 Jerusalem, Israel

[2]Institute for Neuro Immune Medicine, Dr. Kiran C. Patel College of Osteopathic Medicine, Nova Southeastern University, Fort Lauderdale, FL, USA

[3]Lead Contact

*Correspondence: ronitsh@ekmd.huji.ac.il

https://doi.org/10.1016/j.isci.2020.100910

ligand-inducible transcription factors that are members of the superfamily of nuclear receptors (Laudet and Gronemeyer, 2002). RA was also shown to activate transcription through peroxisome proliferator-activated receptor (PPAR) β/δ (Shaw et al., 2003), a member of a subclass of receptors, which also include PPARα and PPARγ that are generally activated by fatty acids and metabolites thereof as their ligands (Varga et al., 2011). RAR and PPAR nuclear receptors are classified as type II nuclear receptors, which reside in the nucleus and associate with retinoid X receptors (RXRs) to form heterodimers and bind regulatory regions of specific target genes (Laudet and Gronemeyer, 2002).

The activating ligands for RAR and PPAR receptors are delivered to the nucleus by specific intracellular lipid-binding-proteins (iLBP) (Konoand Arai, 2015). Cellular retinoic-acid-binding proteins (CRABPs) and fatty-acid-binding proteins (FABPs) belong to this iLBP group. CRABP2 binds RA with high affinity and delivers the bound RA to the nucleus, to activate RAR-mediated gene transcription (Budhu and Noy, 2002). The spectrum of ligands that bind to FABPs is similar to the spectrum of ligands required for the activation of PPAR isotypes (Gutierrez-Gonzalez et al., 2002; Hanhoff et al., 2002; Norrisand Spector, 2002; Widstrom et al., 2001). Studies show that ligand binding and delivery by iLBP add a level of complexity to the network of gene activation by nuclear receptors (Amiri et al., 2018).

The expression of CRABP2 in the adult brain is restricted to cholinergic neurons in the basal forebrain, nucleus accumbens, and the pia mater (Zetterstrom et al., 1999), suggesting that additional iLBP may act similar to CRABP2 in the adult brain. In a previous study, we have shown that α-Syn normally binds fatty acids and suggested that it acts as an FABP (Sharon et al., 2001). We have further shown that α-Syn associations with fatty acids are related to its pathogenesis and toxicity in PD (Assayag et al., 2007; Sharon et al., 2003a; Yakunin et al., 2012) and are mediated through activation of RXR and PPARγ (Yakunin et al., 2012, 2014).

Here we show that α-Syn binds RA to translocate to the nucleus and regulate gene transcription through RAR-RXR, PPARγ, and additional nuclear receptor pathways. α-Syn localization to the nucleus is regulated by calreticulin and is leptomycin-B (LMB1) independent. Importantly, we found detrimental effects of RA on α-Syn homeostasis and evidence linking RA-induced α-Syn translocation to disease mechanisms. We conclude that α-Syn interactions with RA signaling pathway relate to the physiology of this protein as well as to its pathogenicity in PD.

RESULTS

Transcription Profiling following Induced α-Syn Expression Reveals Alterations in Activation of Nuclear Receptors

We sought to study the immediate changes in transcription following induced α-Syn expression. To this aim, we generated a doxycycline-inducible α-Syn expressing SH-SY5Y cell line. The expression of α-Syn mRNA was detected following 6 h and protein expression following 12 h from addition of doxycycline to the conditioning medium (Figures 1A and 1B). At 24 h of induced expression, α-Syn immunoreactivity was predominantly nuclear; however, at 72 h the signal obtained for α-Syn by immunocytochemistry (ICC) was both nuclear and cytosolic (Figure 1C).

A transcriptome analysis identified 129 and 258 protein coding genes that were differentially expressed following 24 or 72 h of induced α-Syn expression (respectively; $p < 0.01$). We analyzed the lists of genes, which differentially expressed, for their upstream regulators. The analysis identified specific ligand-activated nuclear receptors that are regulated by α-Syn expression. At 24 h, the transcription activity of RAR appeared to be strongly affected ($p < 0.000001$) and at 72 h, the transcription activity of RAR-RXR was significantly downregulated ($p = 0.0027$) based on differential expression of two of its target genes, cellular retinoic acid binding protein 2 (CRABP2) and retinol binding protein 1 (RBP1). In addition, the transcription activity of PPARγ was upregulated with α-Syn expression, however, with somewhat lower statistical strength (Figure 1D). Importantly, the transcriptome analysis indicated no differences in the expression levels of RARα, β ,γ or PPARγ following 72 h of induced α-Syn expression, suggesting a regulatory effect at the level of transcription activity.

The effect of α-Syn overexpression to downregulate CRABP2 and RBP1 expression was validated in cultured naive SH-SY5Y cells by qPCR. Significantly lower mRNA levels of CRABP2 (∼30%) and RBP1 (∼10%) were detected in SH-SY5Y cells, transiently transfected with human α-Syn cDNA, than in control cells transfected in parallel with a mock plasmid (Figure 1E, mean ± SD of n = 2–3 experiments;

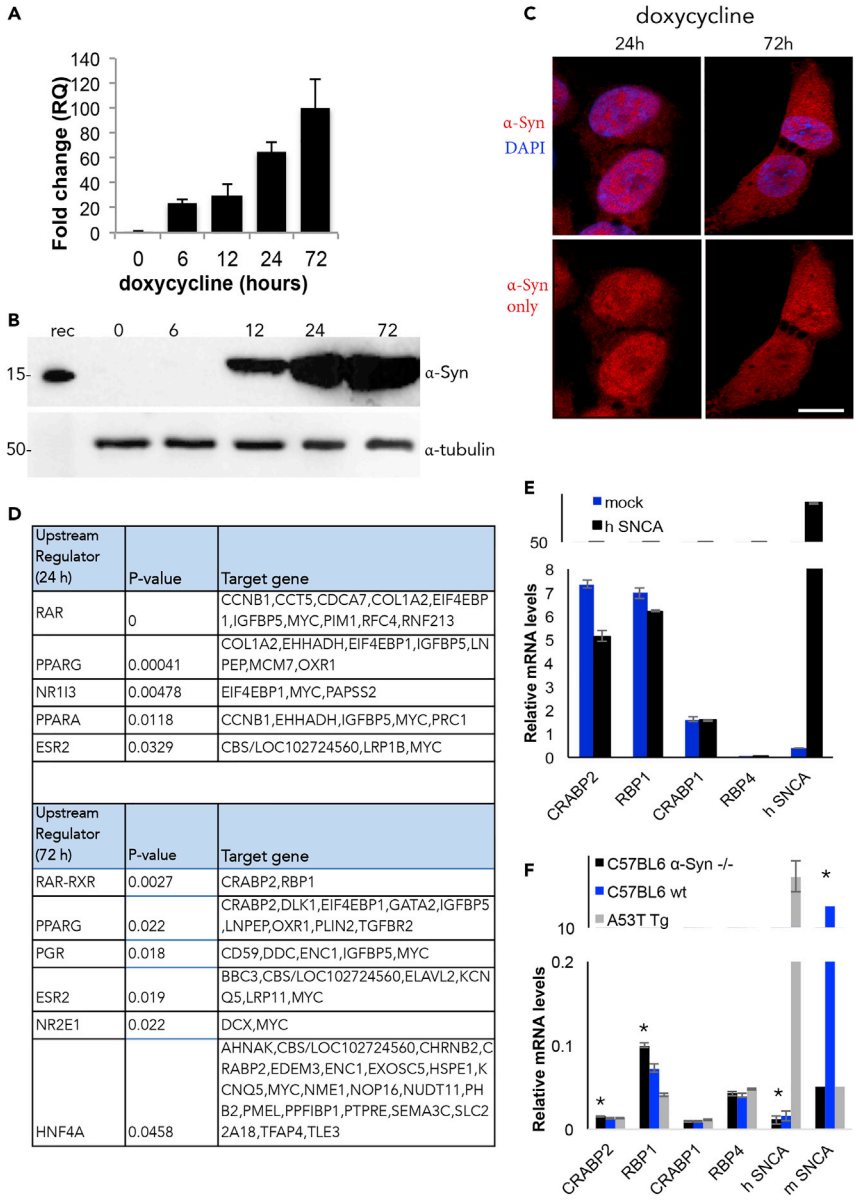

Upstream Regulator (24 h)	P-value	Target gene
RAR	0	CCNB1,CCT5,CDCA7,COL1A2,EIF4EBP1,IGFBP5,MYC,PIM1,RFC4,RNF213
PPARG	0.00041	COL1A2,EHHADH,EIF4EBP1,IGFBP5,LNPEP,MCM7,OXR1
NR1I3	0.00478	EIF4EBP1,MYC,PAPSS2
PPARA	0.0118	CCNB1,EHHADH,IGFBP5,MYC,PRC1
ESR2	0.0329	CBS/LOC102724560,LRP1B,MYC

Upstream Regulator (72 h)	P-value	Target gene
RAR-RXR	0.0027	CRABP2,RBP1
PPARG	0.022	CRABP2,DLK1,EIF4EBP1,GATA2,IGFBP5,LNPEP,OXR1,PLIN2,TGFBR2
PGR	0.018	CD59,DDC,ENC1,IGFBP5,MYC
ESR2	0.019	BBC3,CBS/LOC102724560,ELAVL2,KCNQ5,LRP11,MYC
NR2E1	0.022	DCX,MYC
HNF4A	0.0458	AHNAK,CBS/LOC102724560,CHRNB2,CRABP2,EDEM3,ENC1,EXOSC5,HSPE1,KCNQ5,MYC,NME1,NOP16,NUDT11,PHB2,PMEL,PPFIBP1,PTPRE,SEMA3C,SLC22A18,TFAP4,TLE3

Figure 1. Alterations in Gene Expression following Induced α-Syn Expression

(A) Quantitative PCR (qPCR) detection of α-Syn following its induced expression in SH-SY5Y cells with doxycycline (1 μg/mL; Clontech Laboratories, CA, USA). α-Syn levels normalized to the levels of G6PD gene detected in the same sample. Mean ± SD of n = 4 replicates.

(B)Whole-cell protein lysate of doxycycline-induced α-Syn expressing SH-SY5Y cells (50 μg protein) analyzed by Western blotting and immunoreacted with anti α-Syn antibody, C-20 (Santa Cruz) and α-tubulin, for loading control.

(C) Immunocytochemistry (ICC) following induced α-Syn expression in SH-SY5Y for 24 or 72 hr, using anti α-Syn antibody, C-20 (red). Image shown with (up) or without (down) DAPI for nuclear staining (blue). Bar = 12 μm.

(D) Changes in gene expression analyzed by next-generation whole-transcriptome sequencing (Illumina, CA, USA) and ENSEMBL, for reference genome and annotations. Alterations in transcription activity of specific nuclear receptors analyzed based on changes in expression levels of their target genes, following 24 or 72 h from induced α-Syn expression in SH-SY5Y cells. Analysis performed with Ingenuity Pathway Analysis (IPA) for upstream regulators.

(E) qPCR detection of CRABP2 and RBP1 in naive SH-SY5Y cells following 48 h from transient transfection of human α-Syn or a mock plasmid. No changes in control genes, CRABP1, and RBP4 analyzed in parallel. Data normalized to the expression levels of G6PD (mean ± SD, n = 2–3; *p< 0.01, T test).

(F) qPCR detection of CRABP2 and RBP1 in brains of A53T α-Syn, C57BL/6 α-Syn −/− (a control genetic background for the A53T α-Syn mice), or C57BL/6 WT mice, at 4–5 months of age (mean ± SD, n = 4–6 mice in each genotype; *p< 0.01, T test). Data normalized to the expression levels of 18S gene.

p< 0.01, T test). Similarly, significantly lower mRNA levels of CRABP2 (~18%) and RBP1 (~55%) were detected in young, 4- to 5-month-old, A53T α-Syn than in age- and genetic background (C57BL/6JOlaHsd α-Syn$^{-/-}$) -matched mouse brains (Figure 1F, mean ± SD, n = 4–6; p< 0.01, T test). The two related genes, CRABP1 and RBP4, were used as control genes and in agreement with the transcriptome results their levels of expression did not alter with α-Syn over expression (Figures 1E and 1F).

α-Syn Translocates to the Nucleus in the Presence of RA

We reasoned that α-Syn may translocate to the nucleus in order to regulate RAR-RXR transcription activity. Nuclear translocation of α-Syn was tested following 48 h of doxycycline-induced expression in SH-SY5Y cells. Cells were treated with RA (at 1 or 5 μM) or an equivalent amount of the DMSO solvent (0.1%) for 16 h (see Transparent Methods) before harvest and fractionation. Protein samples of nuclear and cytosolic fractions were analyzed by Western blotting. The quality of the fractions was determined using specific protein markers for nuclear (Lamin B2) or cytosolic (α-Tubulin) fractions. The ratio of α-Syn signal, detected in nuclear to cytosolic fractions, was set at 100% for DMSO-treated cells. Treating SH-SY5Y cells with 1 μM RA had no effect on the nuclear-to-cytosolic signal ratio. However, a significant 147 ± 16% higher signal ratio was detected in cells treated with 5 μM RA (Figures 2A and S1A, mean ± SD of n = 4 different experiments; p< 0.05, T test).

The high concentration of RA (5 μM) required to induce nuclear translocation of α-Syn in SH-SY5Y cells might induce their differentiation. To avoid multiple cellular effects, we next tested α-Syn translocation to the nucleus in the MCF7 cell line, which originated from human breast adenocarcinoma and was commonly used for the study of retinoid signaling. Cells were transiently transfected to express α-Syn and treated with RA (1 μM) or DMSO (0.1%) for 3 h (see Transparent Methods). Cells were collected 48 h post-transfection, fractionated, and analyzed by Western blotting (Figure 2B). Setting the ratio of nuclear to cytosolic α-Syn signal at 100% for DMSO-treated cells, we detected a ~261% higher signal ratio with RA (Figure 2C, mean ± SD of n = 4 different experiments; p< 0.05, T test). The effect of RA to induce nuclear localization of α-Syn was determined by immunocytochemistry (ICC). MCF7 cells were transiently transfected to express α-Syn, treated with RA or DMSO (as above), and processed for ICC with an anti-α-Syn ab (Figures 2D and 2E). α-Syn signal co-localizing with the signal obtained for DAPI was determined as nuclear α-Syn and was extricated from whole-cell α-Syn signal. A significant higher nuclear-to-cytosolic α-Syn signal ratio was detected in cells treated with RA (293%) than those treated with DMSO and set at 100% (mean ± SD of n = 40–44 cells; p< 0.01, T test).

Nuclear translocation of α-Syn in RA- or DMSO-treated MCF7 cells was determined using ImageStream (Figures 2F and 2G). Similarity scores, representing α-Syn signal co-localizing with DAPI as a nuclear marker, were assigned to individual cells. A higher similarity score was detected for α-Syn-expressing cells, treated with RA (0.34 ± 0.02) than cells treated in parallel with DMSO (0.22 ± 0.02) (mean ± SE, n = ~2000 cells). Representative images of cells are shown (Figure 2G).

Translocation of α-Syn to the nucleus in response to RA treatment was verified in primary mesencephalic neurons from wild-type C57BL/6 mouse brains. Cultured neurons (at 10 DIV) were conditioned in medium supplemented with an RA-free serum for 24 h. RA (1 μM) or DMSO (0.1%) were added to the cells for 6 h. Cells were fixed and the nuclear-to-cytosolic signal ratio of endogenous mouse α-Syn was determined by ICC. Importantly, the results obtained in primary neurons confirm the observations in cell lines by showing a significant ~146% higher signal ratio of nuclear to cytosolic α-Syn in RA- than DMSO-treated cells (Figures 2H and 2I; mean ± SD of n = 17–19 cells; p< 0.05, T test).

Additional retinoids, e.g., 13-cis RA and 9-Cis RA, were tested for their effect on nuclear translocation of α-Syn. MCF7 cells were transfected to transiently express α-Syn, treated with the tested retinoids (at 1 μM) for 3 h, and harvested 48 h after DNA transfection. Control cells were conditioned in parallel with DMSO. Following cell fractionation, the nuclear and cytosolic fractions were analyzed by Western blotting and the detected α-Syn levels were normalized to the levels of Lamin B2 and α-tubulin in the same samples (respectively, Figures 2J and S1B). The results show that all three tested retinoids increase nuclear localization of α-Syn with a strongest effect for RA (~4.2 folds), followed by 13-cis RA (~2.9 folds) and 9 cis-RA (~1.9 folds) compared with DMSO (set at 100%; Figure 2K). Attempting to test the specificity of nuclear translocation of α-Syn following its association with small hydrophobic molecules, we tested α-Syn translocation following treatment with fatty acids and found no effect for the tested fatty acids on α-Syn localization to the nucleus (Figure S2A).

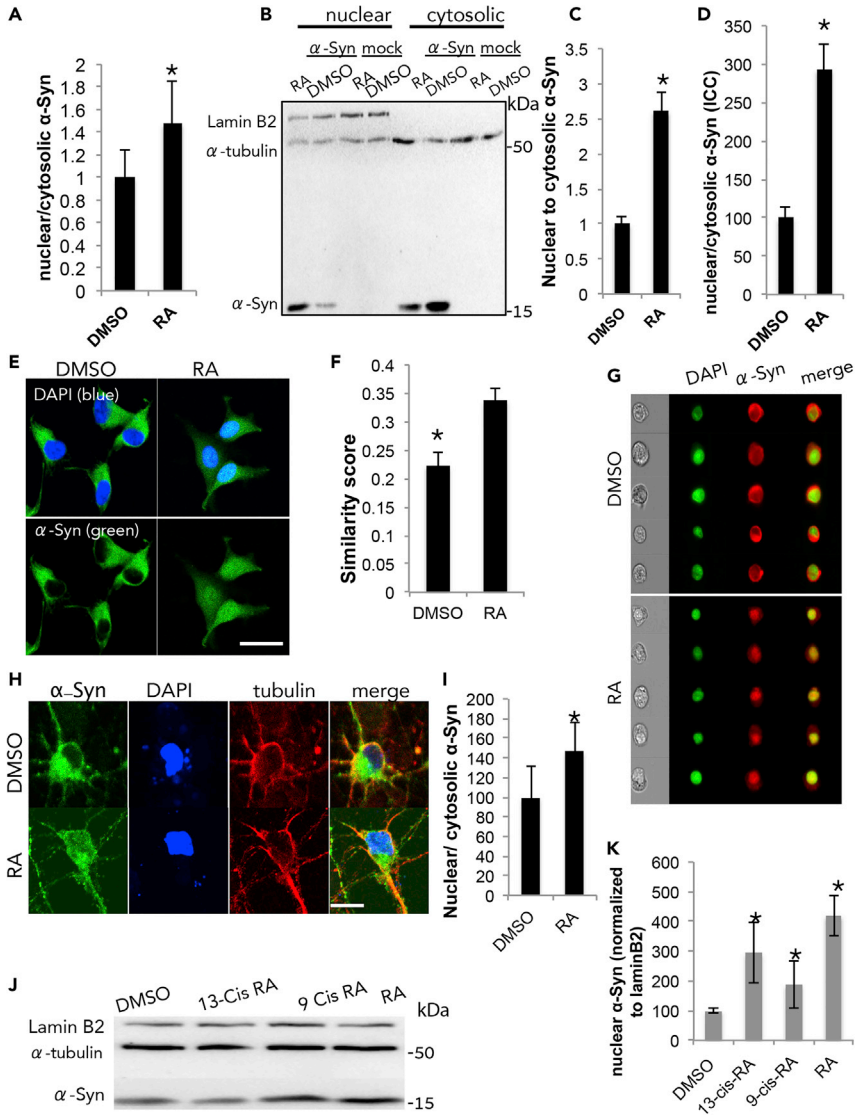

Figure 2. α-Syn Localizes to the Nucleus in the Presence of Retinoic Acid (RA)

(A) Quantitative values representing the nuclear-to-cytosolic ratio of α-Syn signal. α-Syn expression was induced for 48 h in SH-SY5Y cells with 1 μg/mL doxycycline. Cells were treated with RA (5 μM) or an equivalent amount of DMSO (vehicle) for 16 h before harvest. Nuclear and cytosolic fractions were analyzed by Western blotting, immunoreacted with anti α-Syn antibody, C-20; Lamin B2 (nuclear marker); or α-tubulin (cytosolic marker) antibodies. Mean ± SD of n = 4 different experiments; *p< 0.05, T test.

(B) MCF7 cells transiently expressing human α-Syn, treated for 3 h with RA (1 μM) or DMSO solvent and collected 48 h from DNA transfection. The nuclear and cytosolic fractions analyzed by Western blotting and immunoreacted with anti α-Syn, anti α-tubulin, and anti-Lamin B2 antibodies.

(C) Quantitative values of α-Syn signal obtained by Western blotting as in (B), presented as nuclear-to-cytosolic ratio. Mean ± SD of n = 4 different experiments; *p< 0.05, T test.

(D) Quantitative values of nuclear to cytosolic α-Syn signal obtained by immunocytochemistry (ICC). MCF7 cells transfected to express human α-Syn and treated with RA (1 μM) or DMSO for 3 h. Cells fixed 48 h post-DNA-transfection; immunoreacted with anti α-Syn antibody MJF-1 (green), and mounted with a mounting solution containing DAPI (blue). α-Syn signal was quantified by ImageJ. Mean ± SD. N = 40–44 cells; *p< 0.01, T test.

(E) Representative images of MCF-7 cells following immunocytochemistry as described in (D). Bar = 25 μM.

(F) Calculated similarity scores for nuclear localization of α-Syn in MCF7 cells by imaging flow cytometry (ImageStream). MCF7 cells transfected to express α-Syn and treated for 3 h with RA (1 μm) or DMSO. Cells processed for α-Syn detection using anti α-Syn ab (MJF-1) and analyzed for nuclear localization based on the signal obtained with DAPI in the same cell.

Figure 2. *Continued*

A higher similarity score corresponds to a higher degree of nuclear localization of α-Syn. Mean ± SE, n > 1800 cells. *p< 0.01, one way ANOVA. A representative experiment out of n = 3 experiments.

(G) Representative images of MCF7 cells expressing α-Syn (red) and stained with DAPI (green) following 3 h incubation with DMSO (upper panel) or RA (1 μM; lower panel).

(H) Primary mesencephalic neurons from C57BL/6 WT mouse brains (at 10 DIV), conditioned in RA-free medium for 24 h. RA (1 μM) or DMSO added to the cells for 6 h before processing for α-Syn detection by ICC, using anti α-Syn antibody MJF-1 (green) and anti tubulin (red) antibodies. Mounting solution containing DAPI for nuclear staining (blue). Bar = 5 μm.

(I) Quantitative presentation of the results in (H) presenting the ratio of α-Syn signal obtained in nuclear to cytosolic fractions. Mean ± SD of n = 17–19 cells. p< 0.05, T test.

(J) MCF7 cells transfected with human WT α-Syn and treated with either one of the tested retinoids—RA, 9-cis RA, or 13-cis RA (at 1 μM) —or DMSO for 3 h. The nuclear fractions analyzed by Western blotting following immunoreaction with anti α-Syn and anti-Lamin B2 and anti α-tubulin antibodies. A representative blot out of n = 3 experiments.

(K) Quantitative presentation of the analysis in (J); mean ± SD of n = 4 repeats; *p< 0.05, T test.

CRABP2 and α-Syn Compete for Their Nuclear Translocation

CRABP2 normally translocates to the nucleus to deliver RA and activate RAR-dependent transcription (Sesslerand Noy, 2005). MCF7 cells express detectable levels of endogenous CRABP2, yet these levels appear to vary with number of passages. We therefore transiently transfected MCF7 cells to express CRABP2 and treated the cells with RA (1 μM) or an equivalent amount of DMSO for 3 h. Following cell fractionation, protein samples from the nuclear and cytosolic fractions were analyzed by Western blotting. The blot was immunoreacted with specific antibodies for CRABP2, Lamin B2, and α-Tubulin (Figures 3A and 3B). Setting the ratio of nuclear to cytosolic CRABP2 signal in DMSO-treated cells at 100%, we detected ∼230% higher signal in RA-treated cells (mean ± SD of n = 3 experiments; p< 0.01). Similar results were obtained with the endogenous CRABP2 protein.

To find out whether α-Syn and CRABP2 compete for their nuclear translocation following treatment with RA, we co-transfected MCF7 cells to express both proteins. Control cells were transfected with either α-Syn or CRABP2 together with a mock plasmid to maintain constant DNA amounts. Cells were treated with RA or DMSO, fractionated, and analyzed by Western blotting (as above). RA-dependent nuclear CRABP2 signal was calculated as the nuclear-to-cytosolic CRABP2 signal ratio determined in RA- to DMSO-treated cells. This ratio was set at 100% for cells expressing CRABP2 together with the mock plasmid and was ∼50% lower in cells that co-express CRABP2 together with α-Syn (Figures 3C, 3E, and S1C) (mean ± SD of n = 4 experiments; p< 0.05, T test). Similarly, the specific RA-dependent nuclear α-Syn signal was set at 100% for cells expressing α-Syn together with the mock plasmid. A ∼30% lower nuclear α-Syn signal was detected in cells co-expressing α-Syn together with CRABP2 (Figures 3D, 3E, and S1C) (mean ± SD of n = 2–3 experiments; p< 0.05, T test). We concluded that α-Syn and CRABP2 proteins compete for their translocation to the nucleus in the presence of RA.

To find out whether RA affects the expression levels of α-Syn, we utilized primary cortical neurons from C57BL/6 WT mouse brains (Figure 3F). At 10 DIV, cells were conditioned in RA-free medium, supplemented with 1 μM RA or with DMSO (0.1%) for 24 h, to allow transcription before RNA extraction and qPCR analysis. The results show significant ∼129% higher endogenous α-Syn mRNA levels in RA-treated than DMSO-treated cells (mean ± SD of n = 4; p< 0.01). In naive SH-SY5Y human neuroblastoma cells, treated for 24 or 48 h with RA (1 μM) we detected a low, yet, significant increase (∼15%) in endogenous α-Syn mRNA levels, compared with control cells treated in parallel with DMSO (Figure 3G) (mean ± SD of n = 2–3; p< 0.01). In contrast, mRNA levels of CRABP2 were very low in cultured cortical neurons (Zetterstrom et al., 1999) and were not altered following RA treatment (Figure 3F). In control experiment, we verified the effect of RA on mRNA levels of CRABP2 in MCF7 cells and found ∼10 folds higher CRABP2 mRNA levels following 24 and 48 h of RA treatment (Figure 3H) (mean ± SD of n = 4; p< 0.001). Together, RA specifically enhances transcription of α-Syn in neuronal cells.

RA-Induced Nuclear Translocation of α-Syn Involves Transcription Activation

A reporter gene that consists of RAR-response element (RARE) positioned upstream of the open reading frame of luciferase (luc) was used to study the ofα-Syn on transcription activation. MCF7 cells were transfected to co-express RARE-luc and β-galactosidase (β-gal, a control for transfection efficacy) together with either α-Syn or a mock plasmid. Cells were treated with the tested retinoids, RA, 9-cis-RA, or 13-cis-RA (at 50 nM) for 24 h and collected 48 h post-transfection. Control cells were conditioned in parallel with an equivalent amount of DMSO. The results show a specific effect for α-Syn in activating luciferase activity through each of the tested retinoids. The increases in luciferase activity in cells transfected with the

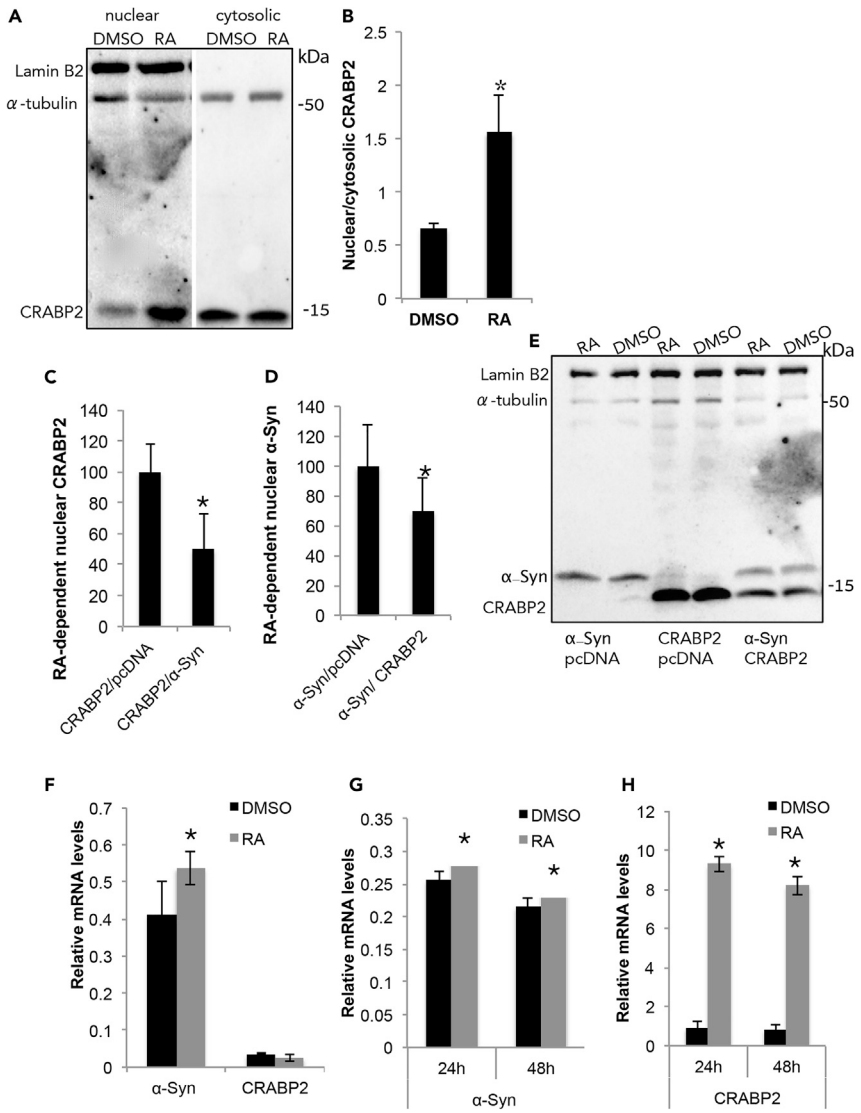

Figure 3. CRABP2 and α-Syn Compete for Their Nuclear Translocation

(A)Western blot analysis of nuclear and cytosolic fractions of MCF7 cells transiently transfected to express CRABP2. Cells treated with RA (1 μM) for 3 h before harvest at 48 h post-DNA-transfection. Control cells treated in parallel with DMSO (vehicle). Blot immunoreacted with anti CRABP2, anti α-Tubulin (a cytosolic marker), and anti-Lamin B2 (a nuclear marker) antibodies.

(B) Quantitative values presenting the nuclear to cytosolic ratio of CRABP2 signal obtained with Western blotting. Mean ± SD of n = 4 experiments; *p< 0.01.

(C) MCF7 cells co-transfected with CRABP2 and either α-Syn or a mock plasmid. Cells treated with RA (1 μM) or DMSO. Quantitative values presenting the nuclear-tocytosolic ratio of CRABP2 signal obtained with Western blotting in RA to DMSO-treated cells. Mean ± SD of n = 4 experiments; *p< 0.01.

(D) MCF7 cells co-transfected with α-Syn and either CRABP2 or a mock plasmid. Cells analyzed as in (C) however, using an anti α-Syn antibody. Mean ± SD of n = 4 experiments; *p< 0.01.

(E) A representative Western blot showing the nuclear fraction of MCF7 cells transiently transfected as indicated. Cells treated as in (A). Immunoblot reacted with antibodies against BRABP2, α-Syn, α-tubulin, and LaminB2.

(F) qPCR detection of endogenous mouse α-Syn and CRABP2 in primary cortical neurons from C57BL/6 WT mouse brain. At 10 DIV cells were treated with RA (1 μM) or DMSO for 24 h to allow transcription before extraction of total RNA. Mean ± SD of n = 4. *p< 0.01, T test.

(G) qPCR detection of endogenous human α-Syn in naive SH-SY5Y cells following treatment of 24 or 48 h with RA (1 μM) or DMSO. Mean ± SD of n = 4; *p< 0.01, T test.

(H) qPCR detection of endogenous CRABP2 in MCF7 cells following treatment of 24 or 48 h with RA (50 nM) or DMSO. Mean ± SD of n = 4; *p< 0.001, T test.

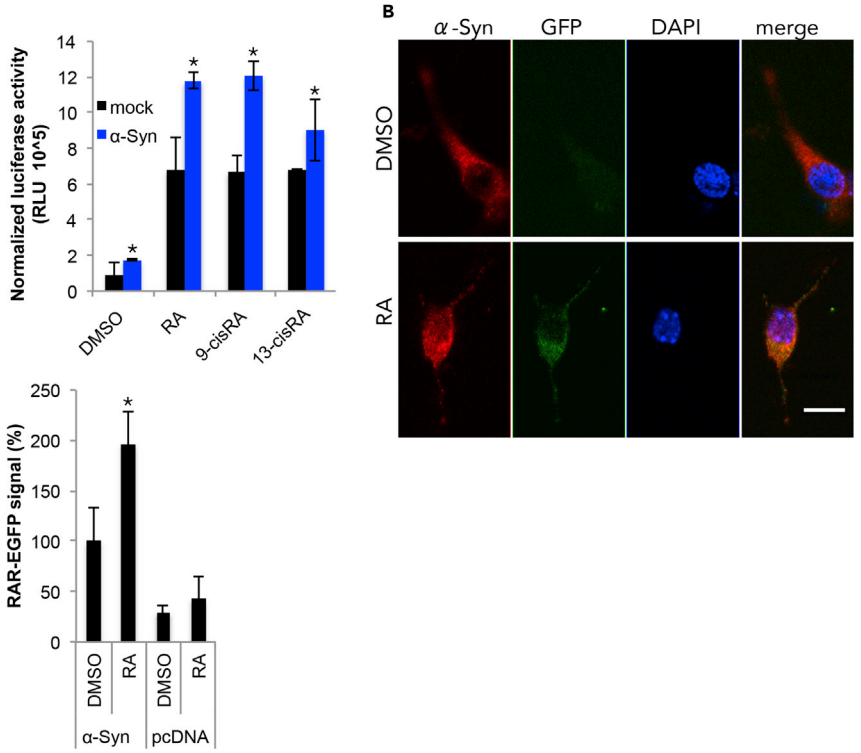

Figure 4. Nuclear Translocation of α-Syn Involves Activation of Gene Expression

(A) MCF7 cells were co-transfected to express α-Syn, RARE-driven luciferase reporter gene, and β-galactosidase (β-gal). Cells were treated with the indicated retinoids (at 50 nM) or DMSO for 24 h and harvested 48 h post-DNA-transfection. Luciferase activity normalized to β-gal activity determined in the same sample. Mean ± SD of n = 4 repeats; *p< 0.05, T test.

(B) Primary cortical neurons from C57BL/6 α-Syn −/− mouse brains, electroporated to co-express RARE-driven GFP reporter gene together with α-Syn or pcDNA (mock) plasmid. At 4 DIV, cultured neurons were treated with RA (50 nM) or DMSO for 24 h and processed for ICC at 48 h post-DNA-transfection. α-Syn immunoreactivity obtained with an anti α-Syn MJF-1 antibody (red); GFP signal (green) captured directly at 488 nm; nuclei stained with DAPI (blue). Bar = 5 μm.

(C) Graph bars depict quantification of the GFP signal in primary cortical neurons as in (B). Mean ± SD of n = 25–30 cells, *p< 0.05, T test.

mock plasmid and treated with retinoids can be explained by the endogenous retinoid system in these cells. α-Syn further enhanced luciferase activity over the mock-transfected cells by ~2-fold with RA or 9-cis RA and by ~1.3-fold with 13-cis RA (Figure 4A, n = 4 different experiments, p< 0.05, T test).

To exemplify RAR activation by α-Syn in primary neurons, we constructed a reporter gene that consists of RARE positioned up-stream of the open reading frame of GFP. Primary cortical neurons prepared from C57BL/6 α-Syn −/− mouse brains were electroporated to express the RARE-GFP construct together with human α-Syn or a pcDNA (mock) plasmid. At 4 DIV cells were treated with 50 nM RA or an equivalent amount of DMSO for 24 h. Cells were fixed and processed for the detection of human α-Syn using an anti α-Syn antibody. A cytosolic GFP signal was clearly detected in RA-treated neurons and was accompanied with a nuclear α-Syn signal. Importantly, a significantly higher GFP signal was detected in cortical neurons treated with RA (209 ± 42%) than in control neurons treated with DMSO (set at 100%; Figures 4B and 4C) (mean ± SD of n = 25–30 cells; p< 0.05, T test). GFP signal in neurons expressing the mock plasmid was not different between RA- and DMSO-treated cells.

α-Syn Binds RA with High Affinity

To determine the affinity of α-Syn to RA we utilized isothermal titration calorimetry (ITC) assay. A heat release curve was obtained following titration of RA (100 μM in 1% DMSO) into a calorimeter cell containing purified α-Syn (10 μM protein in 1% DMSO). Integration of the heat signals (Figure 5A) provided a Kd value of $0.5 \times 10^{-6} \pm 0.24 \times 10^{-6}$ M. At 25°C, the enthalpy (ΔH) was −29.5 ± 17.9 kJ/mol and entropy (TDS) was −3.76 kJ/mol.

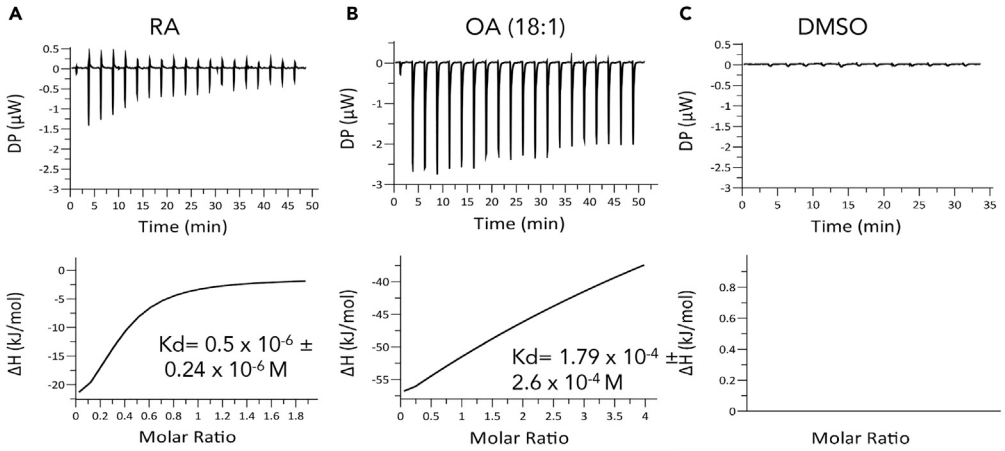

Figure 5. α-SynBinds RA

(A) Isothermal titration calorimetry (ITC) measurements of purified human α-Syn (10 μM) with RA. Reference measurement performed at 25°C in a buffer containing Tris-Cl pH 7.5 and 150 mM NaCl. Both cells contained 1% DMSO solvent.
(B) ITC measurements of α-Syn with oleic acid (OA, 18:1) as in (A) but without DMSO.
(C) ITC measurements showing titration of 1% DMSO to solution containing α-Syn protein.

In a previous study, we have shown that α-Syn binds fatty acids (Sharon et al., 2001). We therefore tested α-Syn binding to oleic acid (OA, 18:1) by ITC. The heat release curve following titration of OA (200 μM) into a calorimeter cell containing α-Syn (10 μM) indicated a low affinity, with a Kd value of $1.79 \times 10^{-4} \pm 2.6 \times 10^{-4}$ M (Figure 5B). Similar affinity was detected for α-Syn with α-linolenic acid (ALA, 18:3), with a Kd of $2.21 \times 10^{-4} \pm 3.6 \times 10^{-4}$ M. Thus, the ITC results show that α-Syn binds RA at a higher affinity than the tested fatty acids. Of note, in the presence of fatty acids, the changes in enthalpy (ΔH, −335 ± 310 kJ/mol) and entropy (TDS, −335 ± 110 kJ/mol) are more pronounced, suggesting differences in structural changes in α-Syn protein upon binding either RA or fatty acids.

In control experiments we titrated RA in the absence of α-Syn (Figure S3) or 1% DMSO to solution containing α-Syn protein (Figure 5C). No changes in heat or in peak intensity in these control experiments were detected.

α-Syn Associations with RA Are Involved in Transcription Activation

To validate a role for α-Syn associations with RA in gene expression we performed a second transcriptome analysis. α-Syn expression was induced for 72 h with doxycycline in inducible SH-SY5Y cells. Cells were treated with RA (5 μM) or DMSO for 16 h before harvested. Sister cultures were treated in parallel with ALA (18:3, 0.25 mM with 0.05 mM BSA) or BSA only (see Supplemental Information) or left untreated in standard serum-supplemented medium. Control cells included the inducible SH-SY5Y cells grown and treated in parallel but without doxycycline and SH-SY5Y cells expressing the trans-activator upstream of a mock plasmid, conditioned with doxycycline.

We identified 2,242 genes that were differentially expressed ($p < 0.05$) in α-Syn-expressing cells treated with RA over DMSO-treated cells. In cells without induced α-Syn expression, we identified 1,110 genes that differentially expressed with RA over DMSO treatment. To elucidate the overall impact of nuclear receptors, we analyzed the lists of genes that differentially expressed using IPA analysis for their upstream regulators (as above). The analysis identified the profile of specific ligand-activated nuclear receptors that are regulated by RA or α-Syn/RA. The nuclear receptors activated with RA treatment were also activated with α-Syn/RA treatment, yet with differences in their degree of activation, represented by the *Z* score and p value of overlap. That is, the transcription activity of RXRα, RARβ, PPARγ, liver X receptor (LXR) α, and thyroid hormone receptor (THR) β was specifically enhanced by RA treatment and furthermore by α-Syn/RA treatment. Estrogen receptor (ESR) 1 was inhibited with RA and furthermore with α-Syn/RA (Figure 6A). In contrast, an opposite trend was obtained for RARα that was activated by RA; however, in α-Syn/RA treated cells the analysis showed a lower degree of activation, represented by a lower *Z* score. Similarly, PPARα and PPARβ/δ were both activated by RA; however, in α-Syn/RA treated cells their pvalues were insignificant (Figure 6A). Of note, the expression levels of RARβ and cyp26A1, two genes that harbor an RARE in their promoter, were activated with RA, and overexpressing α-Syn showed no further activation of their transcription.

A

	α-Syn-RA		RA	
up sream regulator	Z score	P value	Z score	P value
RXRα	3.3	0.000035	2.4	8E-08
RARα	1.2	0.0002	2	6E-09
RARβ	2.9	0.005	2.7	0.0005
PPARα	2.5	0.113	2	0.07
PPARγ	3.7	0.01	2.5	0.0005
PPARδ	2.6	0.08	1.6	0.003
ESR1	-5.3	1E-10	-2.6	2E-08
NR1H3	3.1	0.0006	2.3	0.0002
THRβ	2.4	0.004	1.8	0.001

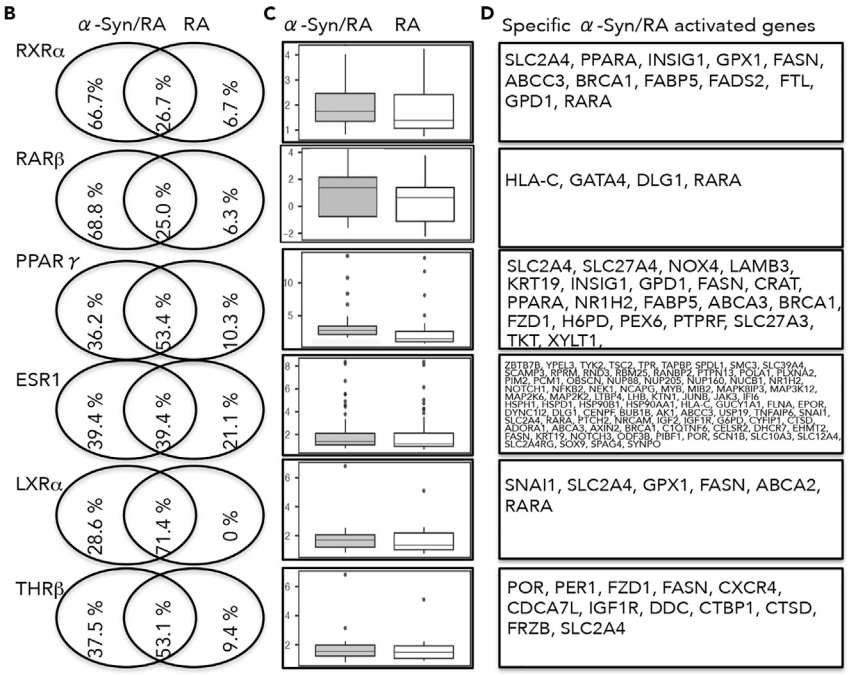

Figure 6. α-SynAssociations with RA Regulate Activation of Nuclear Receptors

(A)α-Syn expression was induced with doxycycline in SH-SY5Y cells for 72 h. Cells were treated for 16 h with RA (5 μM) or DMSO. Control cells were grown and treated in parallel but without induced α-Syn expression. Alterations in transcription were analyzed using next-generation whole-transcriptome sequencing (Illumina, CA, USA) and ENSEMBL, for reference genome and annotations. Lists of differentially expressed genes were analyzed by Ingenuity pathway analysis (IPA) to identify alteration in transcription activity of nuclear receptors (upstream regulators). The nuclear receptors with altered regulation upon α-Syn/RA treatment or RA alone are designated according to their *Z* score (activated >2 or inhibited <−2) and p value of overlap (<0.05). Retinoid X receptor (RXR) α, retinoic acid receptor (RAR) β, peroxisome-proliferator-activated receptor (PPAR) γ, liver X receptor (LXR) α, thyroid hormone receptor (THR) β, and estrogen receptor (ESR) 1.

(B) Venn diagrams showing the distribution of the differentially expressed genes (as in Figure 6A), presented in percent of the altered genes, downstream of each nuclear receptor.

(C) Box plots showing the fold changes in expression of the shared differentially expressed genes in both treatments, RA vs. α-Syn/RA. Presented as log (2) fold change.

(D) List of differentially expressed genes specifically altered by α-Syn associations with RA downstream to the respected nuclear receptor.

To elucidate the molecular signature of α-Syn associations with RA on gene expression we analyzed the lists of differentially expressed genes, assigned to each of the identified nuclear receptor pathways, using Venn diagrams (Figures 6B and S4). For those nuclear receptors that show further activation with α-Syn/RA over RA

alone, the analysis shows that the percent of genes that are differentially expressed exclusively in α-Syn/RA is higher than in RA-only treatment. Among the genes that were altered in both treatments, represented in the overlapped section of the diagram, we found that their fold changes in expression are higher in the α-Syn/RA treatment (Figure 6C). Indicating that α-Syn associations with RA enhanced both the number of differentially expressed genes and the fold changes in gene expression (Figures 6B–6D).

Interestingly, the number of genes that are differentially expressed exclusively in α-Syn/RA over RA alone is also higher for RARα, PPARα, and PPARβ/δ. However, due to differences in the direction of regulation, whether activated or inhibited, the IPA analysis identified an overall insignificant role for α-Syn associations with RA for these nuclear receptors (Figure S4).

α-Syn Associations with Fatty Acids Do Not Enhance Its Nuclear Translocation nor Transcription Activation

In previous studies, we and other groups reported that α-Syn associates with fatty acids (Assayag et al., 2007; Ben Gedalya et al., 2009; Fanning et al., 2019; Golovko et al., 2009; Sharon et al., 2001, 2003a, 2003b). Considering the results indicating alterations in peroxisome-proliferator-activated receptor (PPAR) γ and hepatic nuclear factor (HNF) 4α, two nuclear factors that use fatty acids or metabolites thereof as ligands (Varga et al., 2011; Wisely et al., 2002) (Figure 1D), we thought to find out whether α-Syn associations with fatty acids play a role in its nuclear translocation. To this aim, MCF7 cells were transfected to express α-Syn. Thirty-two hours post-transfection, cells were transferred to a conditioning medium containing 0.1% serum and 0.25 mM fatty acid together with 0.05 mM BSA for 16 h. Control cells expressed α-Syn and conditioned with BSA only. Cells were then fractionated to yield nuclear and cytosolic fractions. Analyzing α-Syn signal ratio in nuclear and cytosolic fractions, we found no significant effect for the tested fatty acids, oleic acid (OA, 18:1), linoleic acid (LA, 18:2), α-linolenic acid (ALA, 18:3) or docosahexaenoic acid (DHA, 22:6), on nuclear localization of α-Syn (Figure S2A). Similar results were obtained in HepG2 cells.

We next asked whether α-Syn associations with fatty acids may interfere with RAR-RXR activation. To this aim, we utilized the RARE-luc reporter plasmid (as in Figure 4A). MCF7 cells were transfected to express RARE-luc reporter plasmid and either α-Syn or a mock plasmid, in addition to β-gal. Cells were conditioned in DMEM supplemented with 0.1% serum and fatty acids (0.25 mM with 0.05 mM BSA) or BSA only (0.05 mM) for 16 h. The results show no effect on luciferase activity, driven by RAR response element, for the tested fatty acids, OA (18:1), LA (18:2), ALA (18:3), or DHA (22:6; Figure S2B).

Similarly, we found no effect for α-Syn associations with fatty acids on activation of reporter genes driven by PPARγ (Figure S2C) or HNF4α response elements (mean ± SD of n = 3–4 experiments).

We performed a transcriptome analysis to analyze a potential involvement of α-Syn associations with fatty acids in gene expression. α-Syn expression was induced for 72 h in SH-SY5Y cells with doxycycline. Sixteen hours before harvest, cells were conditioned in DMEM supplemented with 0.1% serum and α-linolenic acid (ALA 18:3, 0.25 mM with 0.05 mM BSA). Sister cultures were treated in parallel with BSA (0.05 mM) only. Control experiments and analyses were as described in Figure 6.

Differentially expressed protein coding genes that were identified following treatment with ALA (18:3) over BSA-treated cells were analyzed by IPA for their upstream regulators. No specific ligand-activated nuclear receptors met the required cutoff for *Z* score or p value. We concluded that α-Syn associations with fatty acids have no direct effect on its nuclear localization or transcription activation through nuclear receptors.

We concluded that the associations of α-Syn with fatty acids are not involved in its activity to regulate gene expression.

Nuclear Translocation of α-Syn Is Not Affected by Leptomycin B1

Searching for the cellular mechanism that regulates nuclear localization of α-Syn, we tested the effect of leptomycin B1 (LMB1), an inhibitor of CRM-1 exportin (Nishi et al., 1994). MCF7 cells were transfected either with α-Syn or a mock plasmid and treated with RA (1 μM) or DMSO for 3 h in the presence of LMB1. Control cells were treated in parallel with methanol, a solvent for LMB1. Cells were fractionated 48 h post-DNA-transfection and the nuclear fraction was analyzed by Western blotting. The blot was immunoreacted with anti α-Syn, anti Lamin B2, and anti-RanBP1 antibodies. Nuclear levels of endogenous RanBP1 protein

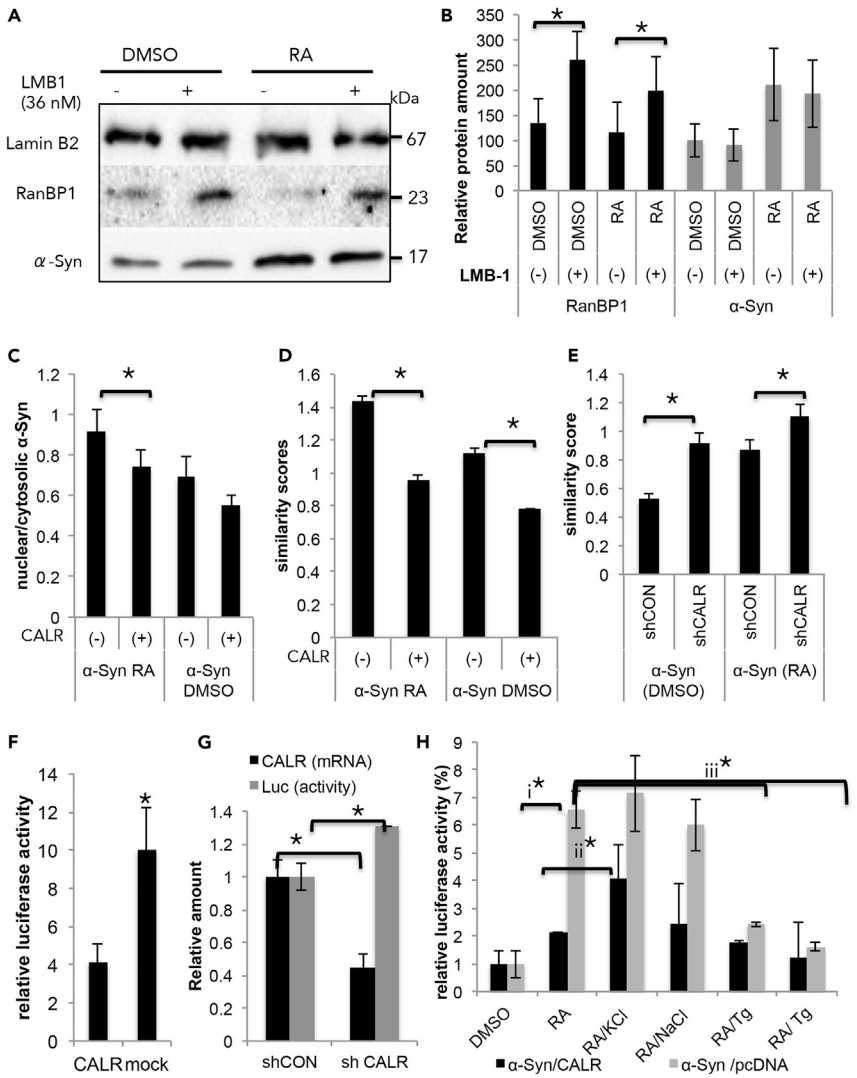

Figure 7. Nuclear Localization of α-Syn Is Calreticulin-Dependent and LMB1-Independent

(A) MCF7 cells transfected with α-Syn plasmid, treated with RA (1 μM) or DMSO together either with LMB1 (36 nM) or methanol (vehicle) for 3 h. Samples of nuclear fraction (50 μg protein) analyzed by Western blotting and immunoreacted with anti α-Syn, anti-Lamin B2, and anti-RanBP1 antibodies. A representative blot out of n = 3.

(B) Quantitative presentation of nuclear levels of α-Syn and RanBP1, normalized to Lamin B2 levels on the same sample. Mean ± SD of n = 2–3 experiments. *p< 0.05, T test.

(C) MCF7 cells transfected to express α-Syn and calreticulin-m-Cherry. Control cells transfected in parallel with α-Syn and a mock plasmid. Cells were treated with RA (1 μM) or DMSO for 3 h and processed for immunocytochemistry with the anti α-Syn ab, MJF-1. Calreticulin signal captured directly through its m-Cherry tag (580 nm, see Figure S5). Nuclear to cytosolic α-Syn signal was quantified in m-Cherry-positive cells by ImageJ. Mean ± SD of n = 20–24 cells; *p< 0.05, T test.

(D) ImageStream fluorescence imaging for nuclear localization of α-Syn based on DAPI signal. Cells transfected and treated as in (C). Mean score ±SD of n >1 000 cells. *p< 0.01, one-way ANOVA. A representative experiment out of n = 3.

(E) MCF7 cells infected with virus particles expressing shRNA for calreticulin (CALR) or a control shRNA (CON) and either α-Syn or a mock plasmids. Five to seven days from the viral infection, cells were treated with RA (1 μM) or DMSO for 3 h. ImageStream fluorescence detection of nuclear localization of α-Syn normalized to total α-Syn signal detected in the cell. Mean similarity score ±SD of n > 600 cells. *p< 0.01, one way ANOVA.

(F) MCF7 cells transfected with four plasmids: RARE-luc, β-gal, α-Syn, and calreticulin (CALR). Control cells were similarly transfected but with a mock plasmid for calreticulin. Cells were treated with RA (50 nm) or DMSO for 24 h. RARE-driven luciferase activity was normalized to β-gal and protein levels and presented as percent of the activity detected in cells expressing calreticulin and treated with DMSO. Mean ± SD of n = 3 experiments. *p< 0.05, T test.

Figure 7. *Continued*

(G) Graph bar showing the relative RARE-driven luciferase activity in plotted against the relative calreticulin mRNA levels in MCF7 cells infected with shRNA for calreticulin (shCALR) or a scrambled control shRNA (shCON); Cells co-express α-Syn and treated with RA (50 nM) for 24 h. Mean ± SD of n = 3 experiments. *p< 0.05, T test.

(H) MCF7 cells transfected and treated with RA or DMSO (as in C). Cell conditioned in the presence of KCl (50 mM), NaCl (50 mM), thapsigargin (Tg, 0.5 μM), or thapsigargin + BAPTA-AM (10 μM). Luciferase activity determined as above. Mean ± SD of n = 3 independent experiments. *p< 0.05, T test.

were used as an internal indicator for effective inhibition of nuclear export by LMB1. The results show that addition of LMB1, up to a concentration of 36 nM, had no effect on nuclear α-Syn levels, whereas under the same experimental conditions, nuclear export of the endogenous RanBP1 protein was inhibited, resulting in higher nuclear RanBP1 levels (Figures 7A and 7B). We concluded that α-Syn localization to the nucleus is CRM-1 independent.

Nuclear Localization of α-Syn Is Regulated by Calreticulin

Calreticulin was shown to play a role in nuclear export of steroid receptors (Burns et al., 1994; Dedhar et al., 1994). We tested the effect of overexpressing calreticulin on nuclear localization of α-Syn in transiently transfected MCF7 cells. Cells were treated with RA (1 μM) or DMSO (0.1%) for 3 h, fixed at 48 h post-DNA-transfection, and processed for ICC using an anti-α-Syn antibody (Figures 7C and S5). The results show a ∼20% lower nuclear-to-cytosolic α-Syn signal ratio in RA-treated cells overexpressing calreticulin compared with cells expressing the mock plasmid. A similar trend was detected in control cells treated with DMSO (n = 25–30 cells, mean ± SD; p< 0.05, T test).

The effect of calreticulin expression on nuclear localization of α-Syn was next tested using ImageStream. Cells were transfected and treated as above (Figure 7C). α-Syn was immunodetected with an anti-α-Syn antibody (at 649 nm). The mean similarity score for RA-treated cells was identified as 0.95 ± 0.03 for cells expressing α-Syn and calreticulin and 1.435 ± 0.02 for cells expressing α-Syn and the mock-plasmid (Figure 7D). The calculated similarity score for DMSO-treated cells was 0.78 ± 0.03 for α-Syn and calreticulin and 1.19 ± 0.02 for α-Syn and the mock-plasmid (mean ± SE N >1000 cells).

We tested the effect of silencing calreticulin on nuclear localization of α-Syn. mRNA levels for calreticulin were ∼60% lower following four days from infecting MCF7 cells with a shRNA virus for calreticulin. These lowered levels were maintained for additional 10 days and experiments were performed during this time window. Analyzing nuclear localization of α-Syn by ImageStream, we detected higher similarity scores, in cells that were treated to downregulate calreticulin expression. That is, the similarity score for RA-treated cells were 0.87 ± 0.03 and 1.05 ± 0.03 in cells expressing control shRNA (shCON) or shRNA for calreticulin (shCALR), respectively. In accord, the similarity score for DMSO-treated cells were 0.52 ± 0.02 and 0.91 ± 0.02, in cells expressing shCON or shCLRT, respectively (Figure 7E).

To find out whether overexpressing calreticulin interferes with transcription activation by α-Syn, we utilized the RARE-luc reporter gene. MCF7 cells were transfected with RARE-luc and α-Syn together either with calreticulin or a mock plasmid. Cells were treated with RA (50 nM) for 24 h, collected 48 h from DNA transfection, and luciferase activity was determined. The results show substantially lower (∼65%) luciferase activity in cells transfected with calreticulin than the mock plasmid (mean ± SD of n = 3 experiments; p< 0.05, T test) (Figure 7F). In accord, α-Syn and RA activation of RARE-luc was ∼30% higher in cells treated to downregulate calreticulin expression than cells expressing the control shRNA (Figure 7G; mean ± SD of n = 3 experiments; p< 0.05, T test).

Calreticulin binds calcium ions and affects cellular calcium homeostasis (Coppolinoand Dedhar, 1998; Michalak et al., 1996, 1999). To find out if calcium plays a role in α-Syn-mediated transcription activation with RA, we utilized the RARE-luc reporter gene (Figure 7H). Cells were transiently transfected to co-express α-Syn either with calreticulin or with a mock plasmid (pcDNA). Twenty-four h post-transfection, the conditioning medium was replaced and cells were conditioned for additional 24 h with RA (50 nM) or DMSO (0.1%) in the presence of either one of the following: KCl (50 mM); NaCl (50 mM); thapsigargin (0.5 μM); or thapsigargin + BAPTA-AM (10 μM). The results confirm the inhibiting effect of calreticulin overexpression on α-Syn/RA luciferase activation (1). Fifty mM KCl partly restored luciferase levels that were downregulated with calreticulin expression (2). However, NaCl at similar concentrations had no such restoring effect, suggesting that increases in cellular calcium levels with KCl overcome calreticulin downregulation.

In accord, lowering cellular calcium levels in α-Syn-/mock-expressing cells with thapsigargin alone or thapsigargin and BAPTA-AM resulted in inhibition of α-Syn/RA-mediated transcription activation (3). The effect of thapsigargin and BAPTA-AM on α-Syn/RA-mediated transcription activation was similar to the effect of calreticulin overexpression. These results therefore suggest that calreticulin effects on α-Syn involve its interactions with calcium.

Finally, in control experiment we tested the potential effect of calreticulin to enhance α-Syn expression levels by qPCR and found no evidence for such an effect. We concluded that calreticulin plays a role in nuclear localization of α-Syn.

Nuclear Localization of α-Syn Is Linked to Parkinson Disease

We reasoned that if α-Syn translocation to the nucleus is linked to its pathogenicity in PD, then the transcriptome analysis should indicate alterations in PD-associated genes. Analyzing the lists of differentially expressed genes following α-Syn expression and RA treatment by IPA, we identified genes that were previously reported to associate with PD (Figure S6). The expression levels of 26 genes that associate with PD were found altered in both conditions, RA only and α-Syn/RA (Figure S6). Three PD-associated genes were differentially expressed specifically with RA treatment. Importantly, the analysis identified eight genes that were altered specifically following α-Syn/RA treatment. These eight genes include two familial PD genes, e.g., ATPase cation-transporting 13A2 (ATP13A2) (Di Fonzo et al., 2007) and PTEN-induced kinase 1 (PINK1) (Valente et al., 2004). In addition, adenosine A1 receptor (ADORA1), dopa decarboxylase (DDC), ferritin light chain (FTL), peptidyl-prolyl isomerase (PIN1), STIP1 homology and U-Box containing protein 1 (STUB1), and poly adenosine 5′-diphosphate-ribose polymerase-1 (PARP-1) were identified.

We next validated a role of α-Syn associations with RA in transcription activation of two of the identified PD-related genes, ATP13A2 and PINK-1. Naive SH-SY5Y cells were infected with α-Syn or a mock vector. Five days post-viral-infection, cells were treated with RA (5 μM) or DMSO for 16 h. The expression levels of ATP13A2, PINK-1, and α-Syn were determined by qPCR and normalized to the expression levels of WPRE, a marker for infectivity and G6PD housekeeping gene (Figure 8A). α-Syn expression was ∼4-fold higher in cells infected with the α-Syn virus than in cells infected with the mock virus. In accord, significantly higher mRNA levels were detected for ATP13A2 (145%) and PINK-1 (∼135%) in the α-Syn-expressing cells, treated with RA than in DMSO-treated cells (set at 100%). To determine α-Syn/RA effect on endogenous ATP13A2 protein levels, we utilized the inducible SH-SY5Y α-Syn-expressing cells. α-Syn expression was induced with doxycycline for 72 h and cells were then treated with RA (5 μM) or DMSO (0.1%) for 16 h. Cells were then incubated for additional 24 h in standard conditioning medium to allow protein translation. Protein samples (25 μg) were analyzed by quantitative Western blotting. ATP132 signal was normalized to tubulin signal and PINK1 signal to HSP60, a mitochondrial marker in the same sample. The results show ∼112% higher ATP13A2 signal and a significant ∼140% higher PINK1 signal in α-Syn/RA than in α-Syn/DMSO cells (Figures 8B–8D) (mean ± SD of n = 4 experiments).

Nuclear translocation of α-Syn with RA was next compared between six of the known PD-associated α-Syn mutations. The nuclear to cytosolic ratio of α-Syn immunoreactivity was determined using ICC in MCF7 cells, transfected to express the different α-Syn cDNAs and treated with RA (1μM) or DMSO for 3 h. Compared with WT α-Syn, significantly higher nuclear-to-cytosolic ratio was detected for A30P, E46K, A53T, and A53E following RA treatment. However, RA-dependent nuclear localization of H50Q and G51D was similar to WT α-Syn (Figure 8E) (mean ± SD of n = 26–53 cells, *p< 0.05, one-way ANOVA).

Alterations in phospho-Ser129 (PSer129) α-Syn levels were next determined as an indicator of α-Syn toxicity following RA treatment. α-Syn expression was induced with doxycycline for 48 h in SH-SY5Y cells and cells were then treated with RA (1 μM) or DMSO for 24 h. Following cell fractionation, a soluble fraction was analyzed for the content of PSer129 α-Syn using a lipid-ELISA assay (see Transparent Methods). The results show significant 182.48 ± 22.5% higher PSer129 α-Syn levels in RA treated than DMSO-treated cells (set at 100%; Figure 8F) (mean ± SD of n = 4 experiments).

Finally, the localization of PSer129 α-Syn to the nucleus, following RA treatment, was tested in primary cortical neurons. Primary cultures were prepared from A53Tα-Syn tg mouse brains. At 14 DIV, cultures were incubated with RA (1 μM) or DMSO (0.1%) for 16 h. Cells were fixed and analyzed by ICC using anti PSer129 α-Syn antibody. Total PSer129 levels and nuclear to cytosolic ratio were determined (Figures

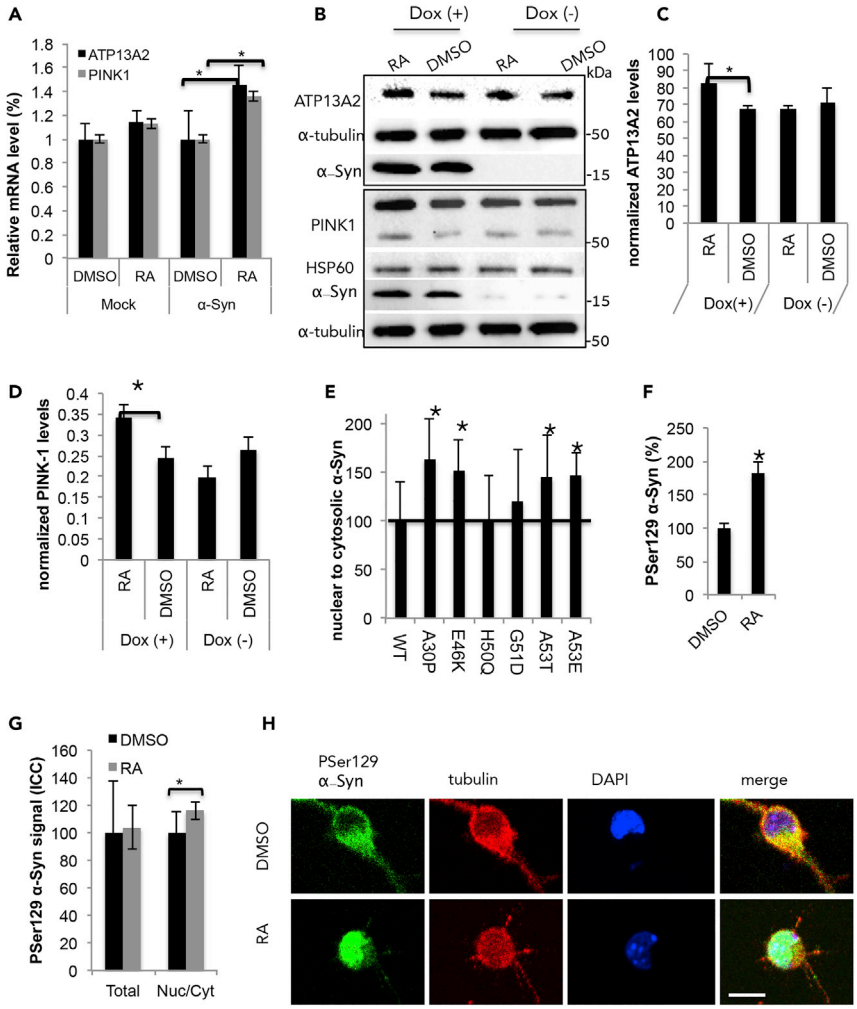

Figure 8. Nuclear Localization of α-Syn Is Linked to Parkinson Disease

(A) qPCR detection of ATPase cation-transporting 13A2 (ATP13A2) and PTEN-induced kinase 1 (PINK1) in SH-SY5Y cells. Cells were transduced to express human α-Syn or a mock-GFP virus and treated for 16 h with RA (5 μM) or DMSO. Cells were collected and analyzed following 5 days from viral infection. Mean ± SD of n = 4 experiments. *p< 0.05 One way ANOVA.

(B) Inducible SH-SY5Y cells conditioned with doxycyline for 72 h to induce α-Syn expression, control cells were conditioned and treated in parallel but without doxycyline. Cells treated with RA (5 μM) or DMSO (0.1%) for 16 h; incubated for additional 24 h in standard conditioning medium and lysed in RIPA buffer. Protein samples (25 μg) were analyzed by quantitative Western blotting. The immunoblot was reacted with the indicated antibodies. Representative blot out of n = 4.

(C) Quantitation of the immunoreactive signal obtained for ATP13A2 (B) normalized to α-tubulin. Mean ± SD. *p< 0.05. One way ANOVA.

(D) Quantitation of the immunoreactive signal obtained for PINK1 (B) normalized to HSP-60. Mean ± SD. *p < 0.05, T test.

(E) MCF7 cells transiently expressing the indicated α-Syn mutations. Cells were treated with RA (1 μM) or DMSO for 3 h and processed for ICC 48 h post-transfection. Bar graph showing the nuclear to cytosolic ratio of each α-Syn form following RA treatment, relative to the respective DMSO-treated cells (WT α-Syn set at 100%, vertical bar). Mean ± SD of n = 26–53. *p< 0.05, one-way ANOVA.

(F) PSer129 α-Syn levels, determined by Lipid-ELISA, in inducible SH-SY5Y cells, conditioned with doxycycline for 48 h, and treated with RA (1 μM) or DMSO for 24 h before cell harvest. The soluble fraction obtained by cell fractionation was analyzed. Mean ± SD of n = 4 experiments. *p< 0.01.

(G) PSer129 α-Syn signal determined in primary cortical neurons from A53T α-Syn at 14 DIV. Neurons incubated with RA (1 μM) or DMSO (0.1%) for 16 h, fixed and analyzed by ICC using anti PSer129 α-Syn antibody. Total PSer129 levels and nuclear to cytosolic ratio are presented. Mean ± SD of n = 15–17 cells. *p< 0.05 T test. (H) ICC of primary cortical neurons immunoreacted with anti PSer129 α-Syn ab (as in (G). An image of the entire neuron is presented in Figure S6).

Bar = 50 μm.

8G, 8H, and S6B). PSer129 α-Syn levels determined in the entire cell varied between cells in both treatments. However, the ratio of cytosolic to nuclear PSer129 α-Syn signal was found to be significantly higher in the RA- (∼116%) than DMSO-treated cells (set at 100%) (mean ± SD of n = 15–17 cells, $p < 0.05$, T test).

DISCUSSION

This study was set to investigate the immediate effects of inducible α-Syn expression on gene transcription. We reasoned that identifying alterations in gene transcription, caused as a function of α-Syn expression, would potentially point at cellular mechanisms directly regulated by α-Syn and provide insights related to the function of this protein. Alterations in transcription of specific nuclear receptors and/or their target genes were identified by whole transcriptome analysis. Downregulation of CRABP2 and RBP1 transcription, two genes regulated by RAR-RXR pathway, suggested to us that α-Syn might play a direct role in retinoid signaling. We found that α-Syn binds RA with high affinity (Kd 0.5 μM) and translocates to the nucleus in a calreticulin-dependent and LMB-1-independent mechanism. Nuclear translocation of α-Syn affected gene transcription through RARs as well as additional nuclear receptors. Importantly, our results show that α-Syn associations with RA are linked to its pathogenicity in PD. RA enhances α-Syn transcription and the accumulation of PSer129 α-Syn toxic form, and α-Syn associations with RA regulate the expression of PD-associated genes. Our results show that α-Syn translocates to the nucleus to deliver RA and highlight a role for α-Syn in retinoid signaling with implications to PD pathogenesis.

We first demonstrated nuclear translocation of α-Syn in SH-SY5Y cells. These cells express dopaminergic markers and are a common cell model for PD. α-Syn translocated to the nucleus with 5 μM RA in SH-SY5Y cells. A lower RA concentration (1 μM) was required to enhance nuclear translocation of α-Syn in the MCF7 cells, which are known for their responsiveness for RA signaling and thus may represent a limitation in using these cells to demonstrate nuclear translocation of α-Syn. Nevertheless, similar to MCF7 cells, nuclear translocation of α-Syn in primary neuronal cultures was achieved with 1 μM RA. The relatively high RA concentration required for nuclear translocation of α-Syn in the SH-SY5Y cells may be part of the retinoid resistance often observed in neuroblastomas (Masetti et al., 2012).

Based on the results herein, we conclude that α-Syn normally and physiologically associates with RA as well as additional retinoids and translocates to the nucleus to activate gene transcription through RAR and RXR nuclear receptors. This conclusion is mainly based on the following two arguments: (1) the choice of an inducible expressing model and the focus on immediate responses to changes in α-Syn expression rather than late, indirect responses; (2) the finding, in primary neuronal cultures, indicating nuclear translocation of endogenous mouse α-Syn in response to RA treatment. In addition, we suggest that in pathogenic conditions, α-Syn associations with RA, its nuclear translocation, or regulation of transcription, are impaired. In support of a pathogenic role for nuclear α-Syn in PD, we show the following: (1) eight PD-associated genes were differentially expressed in cells overexpressing α-Syn and treated with RA; (2) four out of six known PD-causing mutations in α-Syn, tested for their translocation to the nucleus, e.g., A30P, E46K, A53T, and A53E, showed a significant higher degree of nuclear localization compared with WT α-Syn; and (3) α-Syn associations with RA enhanced the accumulation of PSer129 α-Syn form. To better understand the pathogenic aspects of RA-dependent nuclear translocation of α-Syn, it would be interesting to find out whether α-Syn mutations may differ in their affinity to RA; their degree of nuclear receptor activation; and/or their degree of phosphorylation at PSer129 following RA binding. Of relevance, deficiencies in RA or its related pathway of gene transcription have been shown to cause neurodegeneration with PD-like symptoms. Under conditions of vitamin A deficiency, rats became anosmic; mice carrying mutated RARβ and/or RXRγ presented cognitive impairment; and silencing RARα–RXRγ pathway in mice resulted in locomotor impairments (reviewed in Maden, 2007).

Experiments performed using isothermal titration calorimetry (ITC) indicated that α-Syn specifically binds RA (Kd of 0.5×10^{-6} M). It also binds fatty acids, OA (18:1) and ALA (18:3), however, with a substantially lower affinity (Kd 1.79×10^{-4} and 2.21×10^{-4}, respectively). In a previous study, we determined the Kd for α-Syn binding to ^{14}C OA and set it at 0.12×10^{-4} (Sharon et al., 2001). The differences in calculated Kd may result from the methods used. A major advantage of ITC is that it provides direct determination of the association constant (K_a) in solution, by measuring changes in heat upon a binding reaction. Nevertheless, the results presented in Figure 5 suggest that α-Syn binding to RA is different from its binding to fatty acids. Changes in enthalpy and entropy obtained following fatty acid binding suggest structural changes for α-Syn, which were not detected with binding to RA.

We have previously suggested that α-Syn acts as an FABP (Sharon et al., 2001). The finding herein, indicating that α-Syn binds RA with a higher affinity, is reminiscent of FABP5. This family member of the FABP binds an array of ligands in a 1:1 ratio, including fatty acids and fatty acid metabolites of varying carbons chain length and degree of saturation. FABP5 also binds RA and delivers the bound cargo to the nucleus. FABP5 was shown to determine PPARβ/δ-dependent pathway activation through its delivered ligands. That is, the type of the ligand, whether RA, saturated, or unsaturated fatty acids, determined the specific pathway that was activated by PPARβ/δ. Importantly, the partitioning of RA between the two lipid-binding proteins, CRABP2 and FABP5, determined cell fate. That is, RA-mediated activation of RAR supported growth-arrest; however, RA-mediated activation of PPARβ/δ supported cell proliferation (Levi et al., 2015; Schug et al., 2007). We now suggest that similar to FABP5, α-Syn acts in the adult brain to deliver RA from the cytosol to the nucleus to activate gene transcription. However, unlike FABP5, α-Syn does not translocate to the nucleus to deliver fatty acids.

FABPs and CRABPs belong to a family of proteins called intracellular lipid-binding proteins (iLPB). A group of lipid-binding proteins act as intracellular carrier for hydrophobic molecules and target their ligands to specific cellular compartments, including peroxisomes, mitochondria, ER, and the nucleus (Konoand Arai, 2015). The iLBP members share a common structure, consisting of a β-barrel, formed by 10 anti parallel β-strands, containing a ligand-binding N-terminal helix (αI)–turn–helix (αII) motif. This structure is forming a cavity, protecting the hydrophobic molecule from the aqueous environment. iLBP members may bind one or two ligands per molecule of protein. In contrast to the suggested functional similarities between α-Syn and the two iLBPs, CRABP2 and FABP5, there are no known structural similarities between these proteins. α-Syn is known to exist in an equilibrium between a cytosolic, disordered monomer; a membrane-bound form, rich in α-helix structure (Davidson et al., 1998); and oligomeric forms that differ in their structure and degree of toxicity (Fusco et al., 2017).

In respect to CRABP2, our results show that α-Syn expression specifically downregulates its expression and activity. Human CRAPB2 shares 74% amino acid identity with human CRABP1, nevertheless, the CRABPs differ in their function. Although CRABP1 retains the bound RA in the cytoplasm, CRABP2 binds the RA in the cytoplasm and then translocates to deliver the bound RA to the nucleus and activate gene transcription (Wei, 2016). According to the results herein, similar to CRABP2, α-Syn acts to deliver RA to the nucleus for the purpose of transcription activation. The functional similarities between α-Syn and CRABP2 may underlie the findings indicating downregulation of CRABP2 but not CRABP1 expression upon α-Syn overexpression. Accordingly, the effect of α-Syn to specifically downregulate CRABP2 expression may represent compensating mechanisms, designed to cope with α-Syn toxicity, through inhibition of a parallel cellular mechanism with a similar activity. Of note, both CRABP proteins appear to have a high affinity to RA. The reported affinity of CRABP2 (0.13 nM) (Dong et al., 1999) to RA appears higher than the affinity we determined for α-Syn (0.5 μM, Figure 5). Thus, further investigation is needed to understand the competition between α-Syn and CRABP protein. Interestingly, upon translocation to the nucleus, CRABP2 uses hidden nuclear localization signals (NLS), which emerges following ligand-induced change in its tertiary structure (Sesslerand Noy, 2005). In the absence of an identified NLS or a nuclear export signal (NES) for α-Syn, it is possible that similar to the case of CRABP2, structural changes in α-Syn protein may present a functional NLS.

We show that α-Syn localization to the nucleus is regulated by calreticulin and is independent of CRM1, the export receptor for Leucine-rich NES (Nishi et al., 1994). Overexpressing calreticulin resulted in a lower degree of nuclear α-Syn, and downregulating calreticulin resulted in a low, yet, consistent increase in nuclear α-Syn. Calreticulin is an abundant ER luminal calcium-binding chaperone, with established roles in protein quality control and calcium homeostasis (Coppolinoand Dedhar, 1998; Michalak et al., 1996, 1999). Indeed, we demonstrate and interplay between altered cellular calcium and the effect of calreticulin on α-Syn-dependent gene activation. In recent studies, calreticulin was shown to regulate the nuclear export of glucocorticoid receptor (GR), a nuclear receptor that binds its ligand, glucocorticoid, in the cytosol to translocate it to the nucleus (Holaska et al., 2001). Interestingly, similar to α-Syn, GR lacks a conventional leucine-rich NES (Holaska et al., 2001) and does not respond to LMB1 (Liuand DeFranco, 2000). Calreticulin was shown to bind directly to GR (Holaska et al., 2001, 2002), through its DNA-binding domain (Black et al., 2001; Holaska et al., 2002). In addition, calreticulin was shown to play a role in nuclear export of a second nuclear receptor, the thyroid hormone receptor α1 (TRα)1, which shuttles between the cytoplasm and nucleus upon binding of thyroid hormone (Bunn et al., 2001). However, unlike α-Syn and GR, the -nuclear export of TRα1 is affected by both calreticulin and CRM-1 (Grespin et al., 2008). Our results

herein do not distinguish between two potential valid effects for calreticulin, that is, enhanced nuclear export or inhibited nuclear import; however, based on the above reports, calreticulin's effect on nuclear export of α-Syn is more likely.

The involvement of calreticulin in the nuclear localization of α-Syn suggests a role for calcium regulation in this mechanism. Alterations in calreticulin expression levels are strongly associated with impairment of intracellular calcium homeostasis (Michalak et al., 2009). Of note, alterations in calcium levels are implicated in the pathophysiology of α-Syn. A key pathological feature caused by α-Syn aggregation is the disruption of calcium homeostasis (Caraveo et al., 2014; Goldberg et al., 2012; Guzman et al., 2010; Hurleyand Dexter, 2012; Surmeier et al., 2017), which is implicated in mechanism of PD. Calcium binding at the C-terminus of α-Syn accelerated its oligomerization and aggregation (Rcom-H'cheo-Gauthier et al., 2016). Calcium was shown to influence α-Syn's ability to bind to membranes, however, with opposite reported effects (Lautenschlager et al., 2018; Zhang et al., 2014). The critical involvement of calreticulin in calcium homeostasis combined with the results herein (Figure 7) suggests that calcium itself either directly or indirectly regulates the nuclear localization of α-Syn. The involvement of calcium in this process may explain the inconsistency between the degree of calreticulin silencing obtained with the shRNA (~60%) and the low effect on nuclear α-Syn levels (~30%).

A recent study investigated the effect of human α-Syn expression on gene transcription in primary mouse dopaminergic neurons. A transcriptome analysis pointed at Nurr1 as a key dysregulated target for α-Syn toxicity. Nurr1 forms heterodimers with RXR to activate transcription. Based on its heterodimerization with RXR, an approach to restore Nurr1 activity utilized a specific retinoid agonist for RXR. This study highlighted the potential in specific agonists/antagonists for nuclear receptors, in regulation of α-Syn toxicity in PD (Volakakis et al., 2015). We found no evidence for differential expression of NURR1 following α-Syn/RA or RA-only treatments. However, Ret, a transcriptional target for NURR1 was differentially expressed both by RA and α-Syn/RA. Ret is a protein tyrosine kinase and a critical signal transducing subunit of receptors for glial cell-line-derived neurotrophic factor (GDNF) and related neurotrophic factors (Baloh et al., 2000). Ret expression is critical for development and survival of dopaminergic neurons (Tenenbaum and Humbert-Claude, 2017). The direct involvement of α-Syn in gene expression mediated by RAR and RXR, as well as additional nuclear receptors, holds promise for therapy that will consist of specific agonists or antagonists that will regulate a specific PD-pathogenic pathway.

Limitations of the Study

In this study we have demonstrated the mechanism of α-Syn translocation into the nucleus using SH-SY5Y and MCF-7 cell lines and in primary neuronal cultures, cortical and mesencephalic. However, a limitation of this study is the absence of *in vivo* data. Of note, manipulating RA levels *in vivo*, in the mouse brain, is difficult to achieve under physiological conditions.

METHODS

All methods can be found in the accompanying Transparent Methods supplemental file.

DATA AND CODE AVAILABILITY

The authors confirm that the RNAseq data supporting the findings of this study are available within Supplemental Information.

SUPPLEMENTAL INFORMATION

Supplemental Information can be found online at https://doi.org/10.1016/j.isci.2020.100910.

ACKNOWLEDGMENTS

The authors would like to thank Prof. Abraham Fainsod and Drs. Reuven Weiner and Alex Rouvinski for helpful advice in study design and data interpretation. This study was funded by the Israel Science Foundation (ISF) grant 182/12.

AUTHOR CONTRIBUTIONS

D.D. lead the project and performed experiments; M.S., S.AE., and A.M. performed experiments. L.N. designed and performed experiments; R.S. conceived the project and wrote the manuscript.

DECLARATION OF INTERESTS

The authors declare that they have no competing interests.

Received: October 23, 2019
Revised: January 6, 2020
Accepted: February 10, 2020
Published: March 27, 2020

REFERENCES

Al-Wandi, A., Ninkina, N., Millership, S., Williamson, S.J., Jones, P.A., and Buchman, V.L. (2010). Absence of alpha-synuclein affects dopamine metabolism and synaptic markers in the striatum of aging mice. Neurobiol. Aging *31*, 796–804.

Amiri, M., Yousefnia, S., Forootan, F.S., Peymani, M., Ghaedi, K., and Esfahani, M.H.N. (2018). Diverse roles of fatty acid binding proteins (FABPs) in development and pathogenesis of cancers. Gene *676*, 171–183.

Assayag, K., Yakunin, E., Loeb, V., Selkoe, D.J., and Sharon, R. (2007). Polyunsaturated fatty acids induce alpha-synuclein-related pathogenic changes in neuronal cells. Am. J. Pathol. *171*, 2000–2011.

Baloh, R.H., Enomoto, H., Johnson, E.M., Jr, and Milbrandt, J. (2000). The GDNF family ligands and receptors - implications for neural development. Curr. Opin. Neurobiol. *10*, 103–110.

Ben Gedalya, T., Loeb, V., Israeli, E., Altschuler, Y., Selkoe, D.J., and Sharon, R. (2009). Alpha-synuclein and polyunsaturated fatty acids promote clathrin-mediated endocytosis and synaptic vesicle recycling. Traffic *10*, 218–234.

Black, B.E., Holaska, J.M., Rastinejad, F., and Paschal, B.M. (2001). DNA binding domains in diverse nuclear receptors function as nuclear export signals. Curr. Biol. *11*, 1749–1758.

Budhu, A.S., and Noy, N. (2002). Direct channeling of retinoic acid between cellular retinoic acid-binding protein II and retinoic acid receptor sensitizes mammary carcinoma cells to retinoic acid-induced growth arrest. Mol.Cell. Biol. *22*, 2632–2641.

Bunn, C.F., Neidig, J.A., Freidinger, K.E., Stankiewicz, T.A., Weaver, B.S., Mcgrew, J., and Allison, L.A. (2001). Nucleocytoplasmic shuttling of the thyroid hormone receptor alpha. Mol. Endocrinol. *15*, 512–533.

Burns, K., Duggan, B., Atkinson, E.A., Famulski, K.S., Nemer, M., Bleackley, R.C., and Michalak, M. (1994). Modulation of gene expression by calreticulin binding to the glucocorticoid receptor. Nature *367*, 476–480.

Burre, J., Sharma, M., Tsetsenis, T., Buchman, V., Etherton, M.R., and Sudhof, T.C. (2010). Alpha-synuclein promotes SNARE-complex assembly in vivo and in vitro. Science *329*, 1663–1667.

Canete, A., Cano, E., Munoz-Chapuli, R., and Carmona, R. (2017). Role of vitamin A/retinoic acid in regulation of embryonic and adult hematopoiesis. Nutrients *9*, E159–E180.

Caraveo, G., Auluck, P.K., Whitesell, L., Chung, C.Y., Baru, V., Mosharov, E.V., Yan, X., Ben-Johny, M., Soste, M., Picotti, P., et al. (2014). Calcineurin determines toxic versus beneficial responses to alpha-synuclein. Proc. Natl. Acad. Sci. U S A *111*, E3544–E3552.

Coppolino, M.G., and Dedhar, S. (1998). Calreticulin. Int. J. Biochem. Cell Biol. *30*, 553–558.

Davidson, W.S., Jonas, A., Clayton, D.F., and George, J.M. (1998). Stabilization of alpha-synuclein secondary structure upon binding to synthetic membranes. J. Biol. Chem. *273*, 9443–9449.

Decressac, M., Kadkhodaei, B., Mattsson, B., Laguna, A., Perlmann, T., and Bjorklund, A. (2012). alpha-Synuclein-induced down-regulation of Nurr1 disrupts GDNF signaling in nigral dopamine neurons. Sci. Transl. Med. *4*, 163ra156.

Dedhar, S., Rennie, P.S., Shago, M., Hagesteijn, C.Y., Yang, H., Filmus, J., Hawley, R.G., Bruchovsky, N., Cheng, H., Matusik, R.J., et al. (1994). Inhibition of nuclear hormone receptor activity by calreticulin. Nature *367*, 480–483.

Di Fonzo, A., Chien, H.F., Socal, M., Giraudo, S., Tassorelli, C., Iliceto, G., Fabbrini, G., Marconi, R., Fincati, E., Abbruzzese, G., et al. (2007). ATP13A2 missense mutations in juvenile parkinsonism and young onset Parkinson disease. Neurology *68*, 1557–1562.

Dong, D., Ruuska, S.E., Levinthal, D.J., and Noy, N. (1999). Distinct roles for cellular retinoic acid-binding proteins I and II in regulating signaling by retinoic acid. J. Biol. Chem. *274*, 23695–23698.

Eschbach, J., Von Einem, B., Muller, K., Bayer, H., Scheffold, A., Morrison, B.E., Rudolph, K.L., Thal, D.R., Witting, A., Weydt, P., et al. (2015). Mutual exacerbation of peroxisome proliferator-activated receptor gamma coactivator 1alpha deregulation and alpha-synuclein oligomerization. Ann. Neurol. *77*, 15–32.

Fanning, S., Haque, A., Imberdis, T., Baru, V., Barrasa, M.I., Nuber, S., Termine, D., Ramalingam, N., Ho, G.P.H., Noble, T., et al. (2019). Lipidomic analysis of alpha-synuclein neurotoxicity identifiesstearoyl CoA desaturase as a target for Parkinson treatment. Mol.Cell *73*, 1001–1014.e8.

Fares, M.B., Ait-Bouziad, N., Dikiy, I., Mbefo, M.K., Jovicic, A., Kiely, A., Holton, J.L., Lee, S.J., Gitler, A.D., Eliezer, D., and Lashuel, H.A. (2014). The novel Parkinson's disease linked mutation G51D attenuates in vitro aggregation and membrane binding of alpha-synuclein, and enhances its secretion and nuclear localization in cells. Hum. Mol. Genet. *23*, 4491–4509.

Fusco, G., Chen, S.W., Williamson, P.T.F., Cascella, R., Perni, M., Jarvis, J.A., Cecchi, C., Vendruscolo, M., Chiti, F., Cremades, N., et al. (2017). Structural basis of membrane disruption and cellular toxicity by alpha-synuclein oligomers. Science *358*, 1440–1443.

Goers, J., Manning-Bog, A.B., Mccormack, A.L., Millett, I.S., Doniach, S., DiMonte, D.A., Uversky, V.N., and Fink, A.L. (2003). Nuclear localization of alpha-synuclein and its interaction with histones. Biochemistry *42*, 8465–8471.

Goldberg, J.A., Guzman, J.N., Estep, C.M., Ilijic, E., Kondapalli, J., Sanchez-Padilla, J., and Surmeier, D.J. (2012). Calcium entry induces mitochondrial oxidant stress in vagal neurons at risk in Parkinson's disease. Nat. Neurosci. *15*, 1414–1421.

Golovko, M.Y., Barcelo-Coblijn, G., Castagnet, P.I., Austin, S., Combs, C.K., and Murphy, E.J. (2009). The role of alpha-synuclein in brain lipid metabolism: a downstream impact on brain inflammatory response. Mol.Cell.Biochem. *326*, 55–66.

Grespin, M.E., Bonamy, G.M., Roggero, V.R., Cameron, N.G., Adam, L.E., Atchison, A.P., Fratto, V.M., and Allison, L.A. (2008). Thyroid hormone receptor alpha1 follows a cooperative CRM1/calreticulin-mediated nuclear export pathway. J. Biol. Chem. *283*, 25576–25588.

Gutierrez-Gonzalez, L.H., Ludwig, C., Hohoff, C., Rademacher, M., Hanhoff, T., Ruterjans, H., Spener, F., and Lucke, C. (2002). Solution structure and backbone dynamics of human epidermal-type fatty acid-binding protein (E-FABP). Biochem. J. *364* (Pt 3), 725–737.

Guzman, J.N., Sanchez-Padilla, J., Wokosin, D., Kondapalli, J., Ilijic, E., Schumacker, P.T., and Surmeier, D.J. (2010). Oxidant stress evoked by pacemaking in dopaminergic neurons is attenuated by DJ-1. Nature *468*, 696–700.

Hanhoff, T., Lucke, C., and Spener, F. (2002). Insights into binding of fatty acids by fatty acid binding proteins. Mol.Cell.Biochem. *239*, 45–54.

Holaska, J.M., Black, B.E., Love, D.C., Hanover, J.A., Leszyk, J., and Paschal, B.M. (2001). Calreticulin Is a receptor for nuclear export. J.Cell Biol. *152*, 127–140.

Holaska, J.M., Black, B.E., Rastinejad, F., and Paschal, B.M. (2002). Ca2+-dependent nuclear export mediated by calreticulin. Mol.Cell. Biol. *22*, 6286–6297.

Hurley, M.J., and Dexter, D.T. (2012). Voltage-gated calcium channels and Parkinson's disease. Pharmacol.Ther. *133*, 324–333.

Kono, N., and Arai, H. (2015). Intracellular transport of fat-soluble vitamins A and E. Traffic *16*, 19–34.

Kontopoulos, E., Parvin, J.D., and Feany, M.B. (2006). Alpha-synuclein acts in the nucleus to inhibit histone acetylation and promote neurotoxicity. Hum. Mol. Genet. *15*, 3012–3023.

Laudet, V., and Gronemeyer, H. (2002). The Nuclear Receptor FactsBook (Academic Press).

Lautenschlager, J., Stephens, A.D., Fusco, G., Strohl, F., Curry, N., Zacharopoulou, M., Michel, C.H., Laine, R., Nespovitaya, N., Fantham, M., et al. (2018). C-terminal calcium binding of alpha-synuclein modulates synaptic vesicle interaction. Nat. Commun. *9*, 712.

Levi, L., Wang, Z., Doud, M.K., Hazen, S.L., and Noy, N. (2015). Saturated fatty acids regulate retinoic acid signalling and suppress tumorigenesis by targeting fatty acid-binding protein 5. Nat. Commun. *6*, 8794.

Liu, J., and Defranco, D.B. (2000). Protracted nuclear export of glucocorticoid receptor limits its turnover and does not require the exportin 1/CRM1-directed nuclear export pathway. Mol. Endocrinol. *14*, 40–51.

Liu, X., Lee, Y.J., Liou, L.C., Ren, Q., Zhang, Z., Wang, S., and Witt, S.N. (2011). Alpha-synuclein functions in the nucleus to protect against hydroxyurea-induced replication stress in yeast. Hum. Mol. Genet. *20*, 3401–3414.

Maden, M. (2007). Retinoic acid in the development, regeneration and maintenance of the nervous system. Nat. Rev. Neurosci. *8*, 755–765.

Maroteaux, L., Campanelli, J.T., and Scheller, R.H. (1988). Synuclein: a neuron-specific protein localized to the nucleus and presynaptic nerve terminal. J. Neurosci. *8*, 2804–2815.

Masetti, R., Biagi, C., Zama, D., Vendemini, F., Martoni, A., Morello, W., Gasperini, P., and Pession, A. (2012). Retinoids in pediatric onco-hematology: the model of acute promyelocytic leukemia and neuroblastoma. Adv. Ther. *29*, 747–762.

Michalak, M., Burns, K., Andrin, C., Mesaeli, N., Jass, G.H., Busaan, J.L., and Opas, M. (1996). Endoplasmic reticulum form of calreticulin modulates glucocorticoid-sensitive gene expression. J. Biol. Chem. *271*, 29436–29445.

Michalak, M., Corbett, E.F., Mesaeli, N., Nakamura, K., and Opas, M. (1999). Calreticulin: one protein, one gene, many functions. Biochem. J. *344* (Pt 2), 281–292.

Michalak, M., Groenendyk, J., Szabo, E., Gold, L.I., and Opas, M. (2009). Calreticulin, a multi-process calcium-buffering chaperone of the endoplasmic reticulum. Biochem. J. *417*, 651–666.

Milanese, C., Cerri, S., Ulusoy, A., Gornati, S.V., Plat, A., Gabriels, S., Blandini, F., DiMonte, D.A., Hoeijmakers, J.H., and Mastroberardino, P.G. (2018). Activation of the DNA damage response in vivo in synucleinopathy models of Parkinson's disease. Cell Death Dis. *9*, 818.

Nishi, K., Yoshida, M., Fujiwara, D., Nishikawa, M., Horinouchi, S., and Beppu, T. (1994). Leptomycin B targets a regulatory cascade of crm1, a fission yeast nuclear protein, involved in control of higher order chromosome structure and gene expression. J. Biol. Chem. *269*, 6320–6324.

Norris, A.W., and Spector, A.A. (2002). Very long chain n-3 and n-6 polyunsaturated fatty acids bind strongly to liver fatty acid-binding protein. J. Lipid Res. *43*, 646–653.

Paiva, I., Pinho, R., Pavlou, M.A., Hennion, M., Wales, P., Schutz, A.L., Rajput, A., Szego, E.M., Kerimoglu, C., Gerhardt, E., et al. (2017). Sodium butyrate rescues dopaminergic cells from alpha-synuclein-induced transcriptional deregulation and DNA damage. Hum. Mol. Genet. *26*, 2231–2246.

Pinho, R., Paiva, I., Jercic, K.G., Fonseca-Ornelas, L., Gerhardt, E., Fahlbusch, C., Garcia-Esparcia, P., Kerimoglu, C., Pavlou, M.A.S., Villar-Pique, A., et al. (2019). Nuclear localization and phosphorylation modulate pathological effects of alpha-synuclein. Hum. Mol. Genet. *28*, 31–50.

Rcom-H'cheo-Gauthier, A.N., Osborne, S.L., Meedeniya, A.C., and Pountney, D.L. (2016). Calcium: alpha-synuclein interactions in alpha-synucleinopathies. Front.Neurosci. *10*, 570.

Rousseaux, M.W., De Haro, M., Lasagna-Reeves, C.A., De Maio, A., Park, J., Jafar-Nejad, P., Al-Ramahi, I., Sharma, A., See, L., Lu, N., et al. (2016). TRIM28 regulates the nuclear accumulation and toxicity of both alpha-synuclein and tau. Elife *5*, https://doi.org/10.7554/eLife.19809.

Schaser, A.J., Osterberg, V.R., Dent, S.E., Stackhouse, T.L., Wakeham, C.M., Boutros, S.W., Weston, L.J., Owen, N., Weissman, T.A., Luna, E., et al. (2019). Alpha-synuclein is a DNA binding protein that modulates DNA repair with implications for Lewy body disorders. Sci. Rep. *9*, 10919.

Schug, T.T., Berry, D.C., Shaw, N.S., Travis, S.N., and Noy, N. (2007). Opposing effects of retinoic acid on cell growth result from alternate activation of two different nuclear receptors. Cell *129*, 723–733.

Sessler, R.J., and Noy, N. (2005). A ligand-activated nuclear localization signal in cellular retinoic acid binding protein-II. Mol.Cell *18*, 343–353.

Sharon, R., Bar-Joseph, I., Frosch, M.P., Walsh, D.M., Hamilton, J.A., and Selkoe, D.J. (2003a). The formation of highly soluble oligomers of alpha-synuclein is regulated by fatty acids and enhanced in Parkinson's disease. Neuron *37*, 583–595.

Sharon, R., Bar-Joseph, I., Mirick, G.E., Serhan, C.N., and Selkoe, D.J. (2003b). Altered fatty acid composition of dopaminergic neurons expressing alpha-synuclein and human brains with alpha-synucleinopathies. J. Biol. Chem. *278*, 49874–49881.

Sharon, R., Goldberg, M.S., Bar-Josef, I., Betensky, R.A., Shen, J., and Selkoe, D.J. (2001). alpha-Synuclein occurs in lipid-rich high molecular weight complexes, binds fatty acids, and shows homology to the fatty acid-binding proteins. Proc. Natl. Acad. Sci. U S A *98*, 9110–9115.

Shaw, N., Elholm, M., and Noy, N. (2003). Retinoic acid is a high affinity selective ligand for the peroxisome proliferator-activated receptor beta/delta. J. Biol. Chem. *278*, 41589–41592.

Surmeier, D.J., Schumacker, P.T., Guzman, J.D., Ilijic, E., Yang, B., and Zampese, E. (2017). Calcium and Parkinson's disease. Biochem.Biophys. Res. Commun. *483*, 1013–1019.

Tenenbaum, L., and Humbert-Claude, M. (2017). Glial cell line-derived neurotrophic factor gene delivery in Parkinson's disease: a delicate balance between neuroprotection, trophic effects, and unwanted compensatory mechanisms. Front.Neuroanat. *11*, *29*.

Valente, E.M., Abou-Sleiman, P.M., Caputo, V., Muqit, M.M., Harvey, K., Gispert, S., Ali, Z., Del Turco, D., Bentivoglio, A.R., Healy, D.G., et al. (2004). Hereditary early-onset Parkinson's disease caused by mutations in PINK1. Science *304*, 1158–1160.

Varga, T., Czimmerer, Z., and Nagy, L. (2011). PPARs are a unique set of fatty acid regulated transcription factors controlling both lipid metabolism and inflammation. Biochim.Biophys. Acta *1812*, 1007–1022.

Varkey, J., Isas, J.M., Mizuno, N., Jensen, M.B., Bhatia, V.K., Jao, C.C., Petrlova, J., Voss, J.C., Stamou, D.G., Steven, A.C., and Langen, R. (2010). Membrane curvature induction and tubulation are common features of synucleins and apolipoproteins. J. Biol. Chem. *285*, 32486–32493.

Vasquez, V., Mitra, J., Hegde, P.M., Pandey, A., Sengupta, S., Mitra, S., Rao, K.S., and Hegde, M.L. (2017). Chromatin-bound oxidized alpha-synuclein causes strand breaks in neuronal genomes in in vitro models of Parkinson's disease. J. Alzheimers Dis. *60* (s1), S133–S150.

Volakakis, N., Tiklova, K., Decressac, M., Papathanou, M., Mattsson, B., Gillberg, L., Nobre, A., Bjorklund, A., and Perlmann, T. (2015). Nurr1 and retinoid X receptor ligands stimulate Ret signaling in dopamine neurons and can alleviate alpha-synuclein disrupted gene expression. J. Neurosci. *35*, 14370–14385.

Wei, L.N. (2016). Cellular retinoic acid binding proteins: genomic and non-genomic functions and their regulation. Subcell.Biochem. *81*, 163–178.

Widstrom, R.L., Norris, A.W., and Spector, A.A. (2001). Binding of cytochrome P450 monooxygenase and lipoxygenase pathway products by heart fatty acid-binding protein. Biochemistry *40*, 1070–1076.

Wisely, G.B., Miller, A.B., Davis, R.G., Thornquest, A.D., Jr., Johnson, R., Spitzer, T., Sefler, A., Shearer, B., Moore, J.T., Miller, A.B., et al. (2002). Hepatocyte nuclear factor 4 is a transcription

factor that constitutively binds fatty acids. Structure *10*, 1225–1234.

Wong, Y.C., and Krainc, D. (2017). alpha-synuclein toxicity in neurodegeneration: mechanism and therapeutic strategies. Nat. Med. *23*, 1–13.

Yakunin, E., Loeb, V., Kisos, H., Biala, Y., Yehuda, S., Yaari, Y., Selkoe, D.J., and Sharon, R. (2012). Alpha-synuclein neuropathology is controlled by nuclear hormone receptors and enhanced by docosahexaenoic acid in a mouse model for Parkinson's disease. Brain Pathol. *22*, 280–294.

Yakunin, E., Kisos, H., Kulik, W., Grigoletto, J., Wanders, R.J., and Sharon, R. (2014). The regulation of catalase activity by peroxisome proliferator-activated receptorγ is affected by α-Synuclein. Ann. Clin. Transl. Neurol. *1*, 145–159.

Zetterstrom, R.H., Lindqvist, E., Mata De Urquiza, A., Tomac, A., Eriksson, U., Perlmann, T., and Olson, L. (1999). Role of retinoids in the CNS: differential expression of retinoid binding proteins and receptors and evidence for presence of retinoic acid. Eur. J. Neurosci. *11*, 407–416.

Zhang, Z., Dai, C., Bai, J., Xu, G., Liu, M., and Li, C. (2014). Ca(2+) modulating alpha-synuclein membrane transient interactions revealed by solution NMR spectroscopy. Biochim.Biophys. Acta *1838*, 853–858.

Zheng, B., Liao, Z., Locascio, J.J., Lesniak, K.A., Roderick, S.S., Watt, M.L., Eklund, A.C., Zhang-James, Y., Kim, P.D., Hauser, M.A., et al. (2010). PGC-1alpha, a potential therapeutic target for early intervention in Parkinson's disease. Sci. Transl. Med. *2*, 52ra73.

iScience, Volume *23*

Supplemental Information

α-Synuclein Translocates to the Nucleus to Activate Retinoic-Acid-Dependent Gene Transcription

Dana Davidi, Meir Schechter, Suaad Abd Elhadi, Adar Matatov, Lubov Nathanson, and Ronit Sharon

Document S1. Supplemental figures and transparent methods

Figure S1. α-Syn localizes to the nucleus in the presence of retinoic acid (RA).

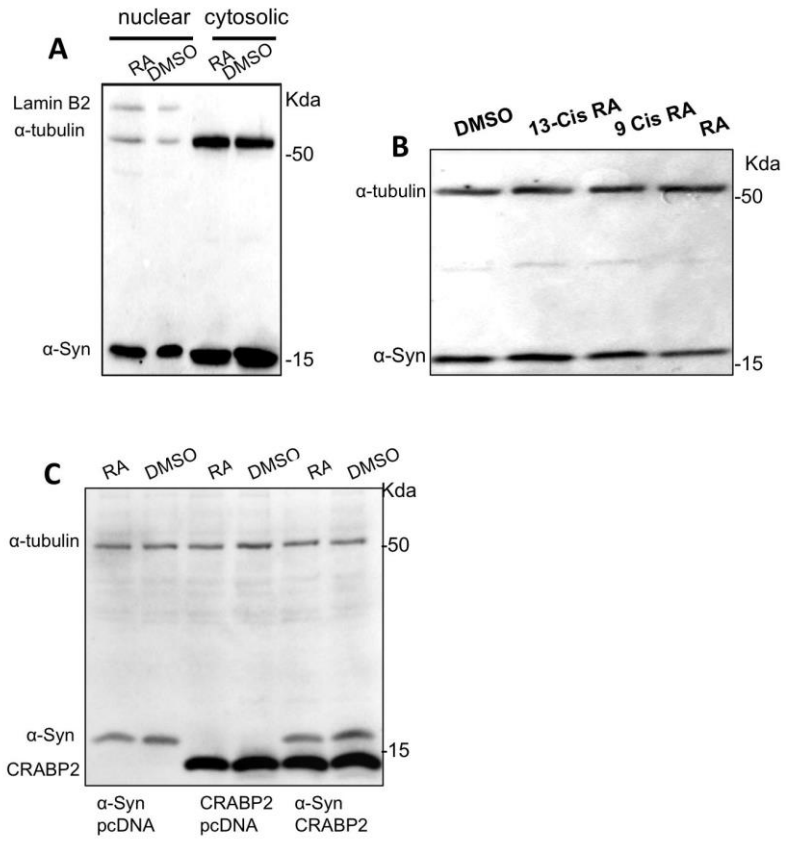

Figure S1. α-Syn localizes to the nucleus in the presence of retinoic acid (RA). Related to Figure 2 and Figure 3.

A. α-Syn expression was induced for 48 hours in SH-SY5Y cells with 1 μg/ml doxycycline. Cells were treated with RA (5 μM) or an equivalent amount of DMSO (vehicle) for 16 hours before harvest. Blot immunoreacted with anti α-Syn antibody, C-20; anti α-tubulin and anti Lamin B antibodies. Representative blot out of n=4.

B. MCF7 cells transfected with human wt α-Syn and treated with either one of the tested retinoids: RA, 9-cis RA, or 13-cis RA (at 1 μM) or DMSO for 3 hours. The cytosolic fractions analysed by Western blotting following immunoreaction with anti α-Syn and anti α-tubulin antibodies. A representative blot out of n=3 experiments.

C. A Western blot analysis of cytosolic fractions as in Fig. 3E.

Figure. S2. α-Syn associations with fatty acids do not enhance its nuclear translocation nor its transcription activation.

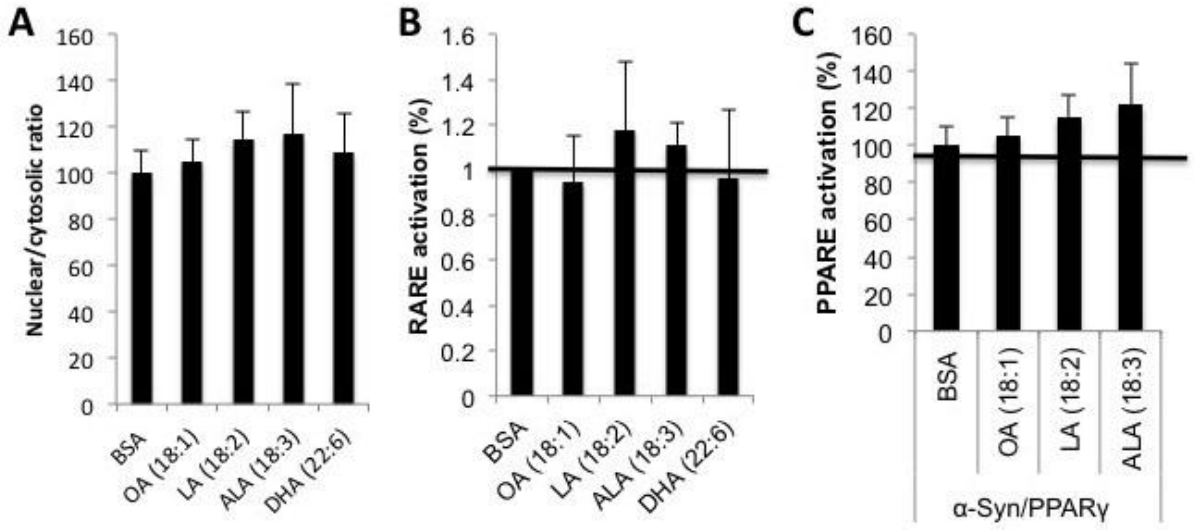

Figure. S2. α-Syn associations with fatty acids do not enhance its nuclear translocation nor its transcription activation. Related to Figure 3.

A. Bar graph showing the results of quantitative values, representing the nuclear to cytosolic ratio of α-Syn signal obtained by Western blotting. MCF7 cells transiently transfected to express α-Syn for 48 hours. Cells were conditioned in DMEM supplemented with 0.1% serum together either with the indicated fatty acids (0.25 mM fatty acid, 0.05 mM BSA) or BSA (0.05 mM) for 16 hours before harvest. Nuclear and cytosolic fractions were analyzed by Western blotting and immunoreacted with anti α-Syn antibody, C-20. Mean ± SD of n= 2 independent experiments.

B. MCF7 cells were co-transfected to express α-Syn, RAR response element (RARE)-driven luciferase reporter gene and β-galactosidase (β-gal) plasmids. Cells were treated with the indicated fatty acids (0.25 mM and 0.05 mM BSA) for 16 hours. Control cells were treated in parallel with BSA only (0.05 mM). Luciferase activity was determined and normalised to β-gal activity and to the protein level in the sample. Vertical bar represents control cells, transfected with a mock plasmid (set at 100%), showing no significant differences. Oleic acid (OA; 18:1), Linoleic acid (LA; 18:2), alpha linolenic acid (ALA; 18:3) and docosahexaenoic acid (DHA; 22:6).

C. MCF7 cells were co-transfected to express α-Syn, PPAR response element (PPARE)-driven luciferase reporter gene, PPARγ2 and β-gal plasmids. Cells were treated with the indicated fatty

acids (0.25 mM with 0.05 mM BSA) or with BSA for 16 hours. Normalized luciferase activity is presented as percent of control cells, that express a mock plasmid and were analysed in parallel (represented by the vertical bar; mean ± SD of n=3-4 experiments).

Figure. S3. α-Syn binds RA.

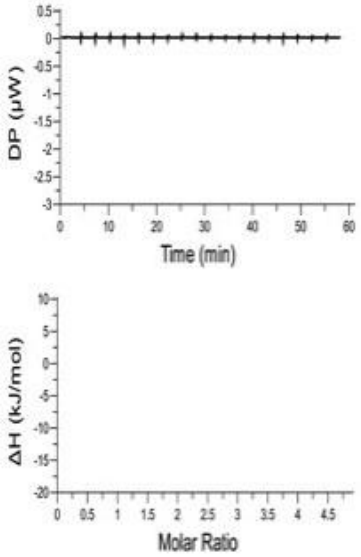

Figure. S3. α-Syn binds RA. Related to Figure 5.

Isothermal titration calorimetry (ITC) measurements showing titration of 100 microM RA in the absence of α-Syn protein.

Figure. S4. Alterations in nuclear receptor activation with RA and α-Syn

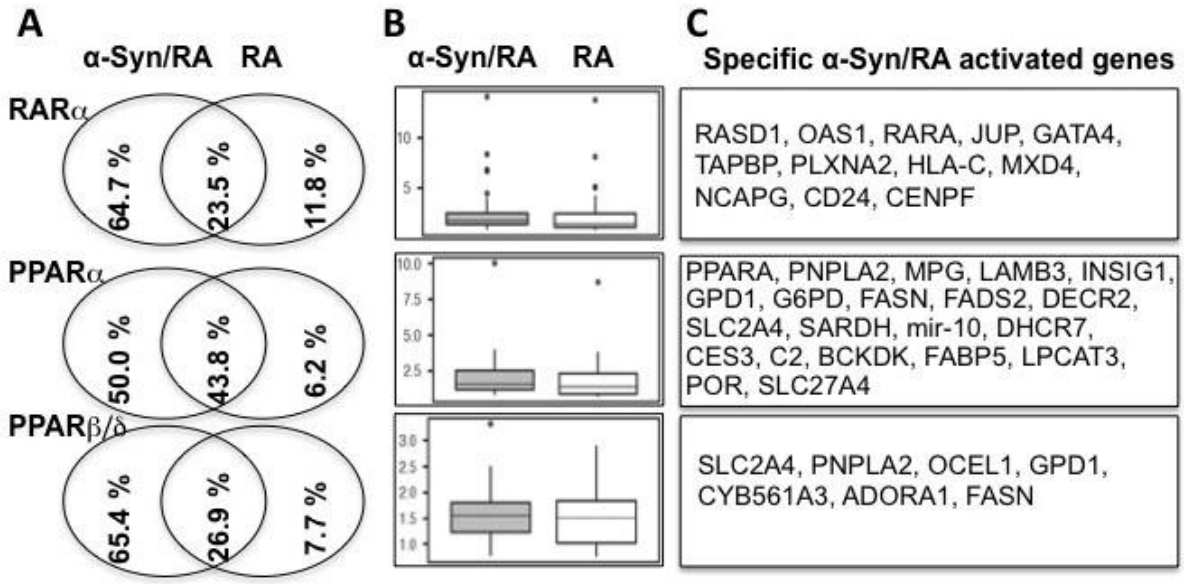

Figure. S4. Alterations in nuclear receptor activation with RA and α-Syn. Related to Figure 6.

A. Venn diagrams showing the distribution of the differentially expressed genes (as in Fig. 6B), presented in percent of the altered genes, down stream of each nuclear receptor.

B. Box plots showing the fold changes in expression of the shared differentially expressed genes in both treatments, RA vs. α-Syn/RA. Presented as log (2) fold change.

C. List of differentially expressed genes specifically altered by α-Syn associations with RA downstream to the respected nuclear factor.

Figure. S5. Nuclear localization of α-Syn is calreticulin-dependent

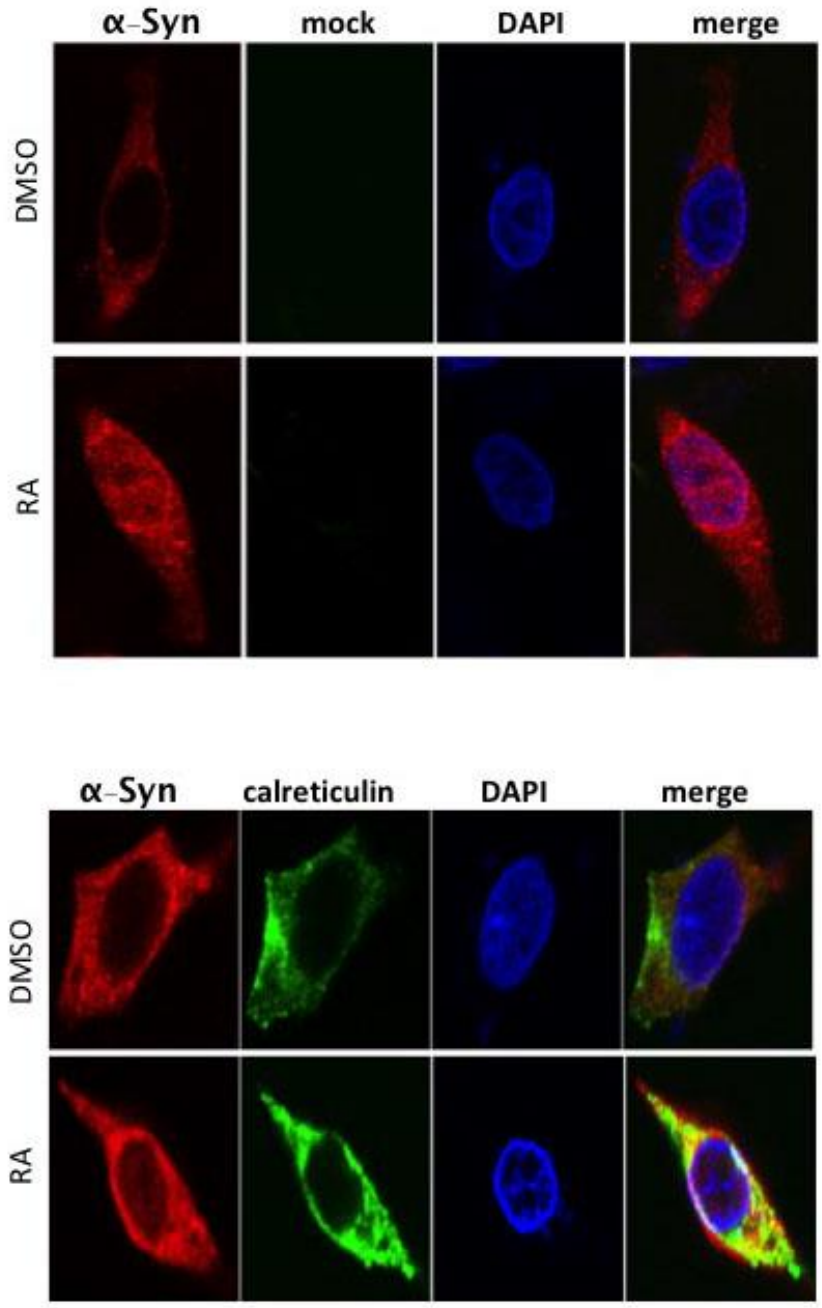

Figure. S5. Nuclear localization of α-Syn is calreticulin-dependent. Related to Figure 7. MCF7 cells transfected to express α-Syn and calreticulin-m-Cherry. Control cells transfected in parallel with α-Syn and a mock plasmid. Cells were treated with RA (1 μM) or DMSO for 3 hours and processed for immunocytochemistry with the anti α-Syn ab, MJF-1. Calreticulin observed directly through its m-Cherry tag (580 nm).

Figure. S6. Nuclear localization of α-Syn is linked to Parkinson's disease

A

α-Syn / RA	RA only	shared
ADORA1	E2F1	ABL1
ATP13A2	KCNH2	ADAMTSL1
DDC	SPP1	ADORA2B
FTL		ADRA2C
PIN1		ANXA2
PINK1		CHRM1
STUB1		CHRM2
PARP-1		CNPCNR1
		DLG2
		GCH1
		LDHA
		MAP1B
		NTRK2
		PDE11A
		PTGS2
		RET
		SCN5A
		SLC6A2
		SNAP25
		SNCA
		STMN1
		SYN2
		TGM2
		TUBA1A
		TUBA1C
		VIM

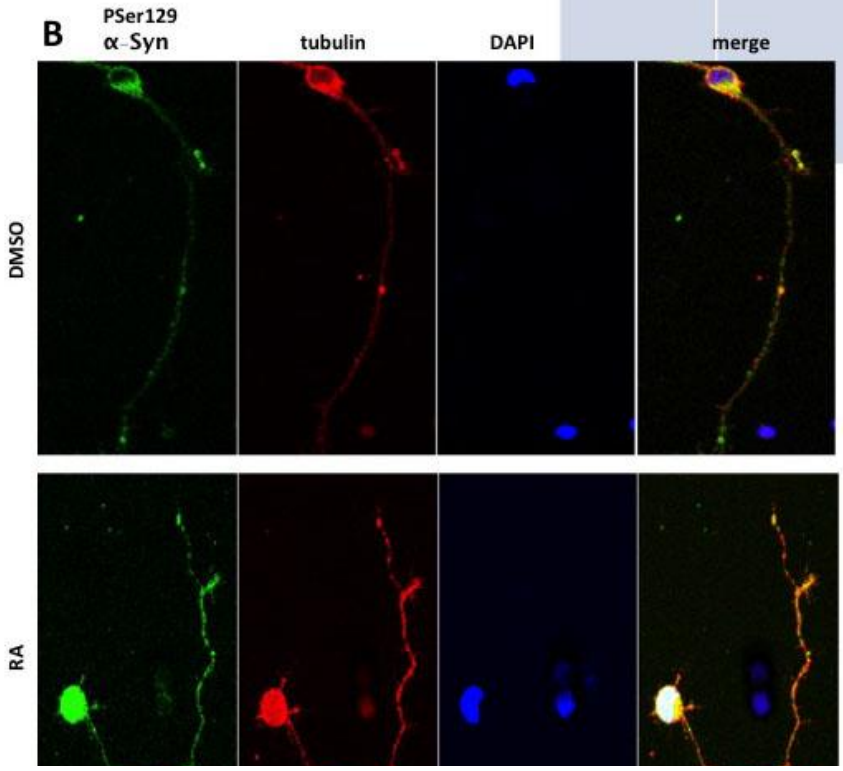

Figure. S6. Nuclear localization of α-Syn is linked to Parkinson's disease. Related to Figure 8.

A. Differentially expressed PD- associated genes identified with IPA analysis in α-Syn/RA or RA-only treated cells, or in both treatments.

B. Primary cortical neurons from A53T α-Syn tg mouse brain at 14 DIV. Neurons treated and immunoreacted with anti PSer129 α-Syn antibody as in Fig. 8H, demonstrating the entire neuronal

cell.

Transparent Methods

Plasmids. RARE-luc plasmid (pGL3-RARE-luciferase) from T. M. Underhill (Addgene plasmid # 13458(Hoffman et al., 2006)); PPARE-luc and PPARγ plasmids from Prof. Yaakov Nahmias (Hebrew University); HNF4RE generated by cloning the sequence of the response element: GGCAAAGGTCATGGCAAAGGTCATGGCAAAGGTCATGGCAAAGGTCATGGCAAAGGTCAT (Sladek et al., 1990) into PGL2 promoter vector (Promega, WI, USA); HNF4α plasmid form Dr. Rachel Hertz (Hebrew University). mCherry-calreticulin from Michael Davidson (Addgene plasmid # #55006). shRNA calreticulin (Mission shRNAi, SHCLNG-NG-004343 Sigma Aldrich).

Inducible α-Syn expression in SH-SY5Y cells. A Tet-On 3G system Tetracycline-Inducible Expression Systems (Clontech Laboratories, CA, USA) was used. Stable clones, expressing either human wt α-Syn or a mock plasmid, downstream of pCMV-Tet 3G plasmid, were generated according to manufacturer instructions. α-Syn expression induced with 1 μg/ml doxycycline (Clontech Laboratories, CA, USA).

RNAseq and analysis for upstream regulators. Total RNA was extracted from confluent 10 cm dishes following 0, 24 and 72 hours (in duplicate) of conditioning the cells in the presence of doxycyline (1 μg/ml, in standard serum-supplemented DMEM), using RNeasy Plus mini kit (Qiagen, Eldan Petach-Tikva, Israel). The quality of the RNA was tested using RNA Analysis Screen-Tape, Agilent 2200 Tape-Station system (Agilent, Eldan, Petach-Tikva, Israel). Library preparations were performed with Truseq RNA kit (Illumina, Danyel Biotech, Rehovot, Israel) from 300 ng of total RNA and analyzed by next generation whole transcriptome sequencing Hiseq, single end sequencing method (Illumina, CA, USA; performed at the Technion Genome Center, Haifa, Israel). Data were analyzed by Fast-QC, for the quality of the raw sequence data and ENSEMBL, for reference genome and annotations. The following analyses were performed: STAR-2.3.0, to align reads to reference genome; Htseq count, for counting number of mapped reads per gene; and DESeq2 package v1.6.3, for normalization and statistical analysis.

RA treatment:

SH-SY5Y cells: Cells were conditioned in DMEM containing 0.1 % serum and RA (1 or 5 μM) or an equivalent amount of the DMSO (0.1%) solvent for 16, 24 or 48 hours before harvest.

MCF7 cells: Cells were conditioned in DMEM containing 0.1% serum (RA starvation) for 16 hours. RA (1μM or 50 nM, as indicated) or 0.1% DMSO, were added to the conditioning medium and cells were conditioned for additional 3 hours. In experiments in which RA treatment was longer than 3 hours we did not starve the cells prior to the treatment.
Primary neurons: 24 hours before harvest, the conditioning medium was replaced to contain medium supplemented with vitamin A-deficient, B27 serum (Biological Industries, Beit Haemek, Israel). RA (1 μM or 50 nM) or DMSO (0.1%) were added to the cells for 6 or 24 hours.

Differential expression following RA or fatty acid treatments

RNA extraction, quality and library preparation was as described above. Illumina HiSeq3000 was used to generate paired-end sequencing with a read length of 150 bp. Minimum 40 million reads were generated per sample. Quality control assessment was done using Illumina RNA-seq pipeline to estimate genomic coverage, percent alignment and nucleotide quality. Raw sequencing data were transformed to fastq format.
Normalization and differential expression were done with the DESeq2 package (version 1.14.1) (Love et al., 2014). The following samples were analyzed: SH-SY5Y cells induced to express α-Syn (with 1 μg/ml doxycycline) and treated for 16 hours in DMEM supplemented with 0.1% serum and either one of the following, RA (5 μM); DMSO (0.1%); ALA (18:3, at 0.25 mM together with 0.05 mM BSA); BSA (0.05 mM) or no treatment (i.e., standard serum-supplemented medium). Cells were collected and analyzed following 72 hours from induction of α-Syn expression. Control samples included an identical set up but without induced α-Syn expression. In addition, the effect of doxycycline on gene expression was tested in induced SH-SY5Y cells expressing a mock plasmid. Total of 12 different treatments, each treatment was tested in triplicate dishes. Normalization with all samples showed that the different treatments had distinct patterns of expression, thus measuring the effect of each treatment was done only with the samples of the relevant treatment. Quality control assays, such as count distributions and principal component analysis, were calculated and visualized in R (version 3.4.1, with packages 'RColorBrewer_1.1-2', 'pheatmap_1.0.8', 'ggplot2_2.2.1' and ggrepel_0.7.0).

The following differential comparisons were performed: A. RA versus DMSO treated cells with induced α-Syn expression; B. RA versus DMSO treated cells without induced α-Syn expression.

Similarly, the effect of fatty acids associations with α-Syn were analyzed by comparing: C. Fatty acids versus BSA treated cells with α-Syn expression; and D. Fatty acids versus BSA without induced α-Syn expression. Then, differential expression was calculated for each system (either RA or fatty acid) with a design of two factors and their interaction as the full model, and omitting the interaction in the reduced model, using the LRT test. The two factors were α-Syn expression (induced or not induced) and the respective treatment (ligand or vehicle). Results were obtained with default parameters, except not using the independentFiltering algorithm, and setting the significance threshold to padj<0.05. The results showed that for many genes, even minor changes were considered significant (probably due to a very high reproducibility between replicates). In order to somewhat filter the results and consider only genes with a stronger effect (fold-change), additional filtering was applied according to the following criterion: significant genes were considered only if their baseMean expression was above 5, and their absolute log2FoldChange was above 5/baseMean^0.5 + 0.6, for the RA system, or 5/baseMean^0.25 + 0.6, for the FA system. This criterion filters genes in an expression-dependent manner, allowing for a fold-change of ~1.5 at very high expression levels, and requiring a fold-change above 7 at the very low expression levels. Only genes that were significant and passed the additional criterion were used in further advanced analysis with IPA (QIAGEN Inc., https://www.qiagenbioinformatics.com/products/ingenuity-pathway-analysis) in order to find enriched pathways, molecular functions and up-stream regulators. IPA® Z-scores greater than 2 or smaller than -2 is considered to be significantly predicted to be up or down- regulated, respectively. P- value of overlap of 0.01 or less is considered significant. Box plots of common downstream genes of each nuclear receptor were generated by ggplot2 R package and its geom boxplot function.

The accession number for the data reported in this paper is GEO: GSE145804

Total RNA extraction and quantitative (q)PCR. Mice (equal numbers of males and females) were anesthetized with isoflurane (2.5%; Piramal Healthcare Limited, Digwal, India). Brains were removed, divided in hemispheres and kept frozen. Total RNA was isolated with TRI-Reagent (MRC, Cincinnati, OH, USA) from one hemisphere of C57BL/6 wt or homozygous PrP-A53T α-

Syn tg mouse brains (Giasson et al., 2002) (Jackson laboratory, Bar Harbor, ME, USA); or from cultured cells, transfected to express human wt α-Syn or a mock plasmid using ICAFectin 411(Incellart, Nantes, France). The RNA was converted to cDNA using High Capacity cDNA, Reverse Transcription Kit (Applied Biosystems, Foster City, CA USA). Primer pairs designed to exon-exon boundaries by Primer3 (v3.0.1 software). Primers sequence is listed in supplementary Table 1. Results were normalized against the expression levels of G6PD (cultured cells of human origin) and 18S for (mouse brains and primary neurons). In experiments in which cells were transduced with lenti virus, results were normalized to the WPRE gene. Analyses were performed using Applied Biosystems Step One Software v2.2.2 with CYBR Green Master Mix (Applied Biosystems Foster City, CA USA).

Cell fractionation, protein extraction and Western blotting. Cultured cells (5x 10^7) collected and spun at 1000 xg. Cell pellet was washed twice in PBS^{++} and re-suspended in 250 µl homogenization (H) buffer [20 mM HEPES, pH 7.4; 1 mM $MgCl_2$; 0.32 M sucrose; 43 mM 2-mercaptoethanol; and 1 x protease inhibitor mix (Sigma-Aldrich, Rehovot, Israel)]. Cells were incubated on ice for 20 minutes and homogenized by eight passages through a 25-gauge needle.

Fractionation: All procedures were performed at 4°C. Cell homogenate was centrifuged at 1,700 xg for 10 min. The supernatant was transferred to a clean tube and spun at 25,000 xg for one hour. The resultant cytosolic fraction was removed to a clean tube. The pellet was washed in H-buffer and re-spun at 1,700 xg for 15 minutes. The washed pellet was re-suspended in H-buffer; brought to 2.1 M sucrose and spun at 25,000 xg for 1 hour. The pellet (consisting of nuclei) was collected, washed and re-suspended in H-buffer containing 1% Nonidet P-40.

Western blotting: Protein samples of cytosolic or nuclear fractions (20 µg) were loaded on a 10% SDS-PAGE and following electrophoresis, proteins were transferred to nitrocellulose membrane (Whatman, Sigma-Aldrich, Rehovot, Israel). The membrane was blotted with an anti α-Syn antibody C-20 (1:2000; Santa Cruz Biotechnology; Petach Tiqva, Israel) or MJF-1 (1:2000, Abcam, Zotal, Tel-Aviv, Israel), anti CRABP2 antibody (1:2000; Millipore, CA, USA), anti Lamin B2 (1:2000; Abcam, ab8983, Zotal, Tel-Aviv, Israel) anti RanBP1 (Abcam, ab8983, Zotal, Tel-Aviv, Israel) or anti α-Tubulin (1:2000; Serotec, Oxford, UK). The immuno-blots were reacted with

a secondary, HRP-conjugated, antibody and visualized with Clarity Western ECL Substrate (Bio-Rad, Rishon Le Zion, Israel), scanned with ChemiDoc XRS^{+} imaging system (Bio-Rad, Rishon Le Zion, Israel) and the density of signal was quantified using UN-SCAN-IT GEL 3.1 software (Silk Scientific, Orem, UT, USA). The quality of fractionation was determined according to the signal obtained for the marker proteins: Lamin B2 for nuclear fraction and α-tubulin for cytosolic fraction.

Immunocytochemistry (ICC). Cultured cells were seeded on cover slides pre-coated with Poly-D Lysine (0.1 mg/ml for 1 hour at 37°C). On the next day doxycycline was added to the conditioning medium to induce α-Syn expression (SH-SY5Y); or cells were transfected as indicated (MCF7 cells). Cells were washed in warm PBS and fixed in 4% paraformaldehyde for 10 minutes on ice. The slides were then blocked in a solution containing 1.5% BSA in PBS. For α-Syn detection, either C-20 ab (1:500; Santa Cruz Biotechnology; Almog Diagnostic, Petach Tiqva, Israel) or MJF-1 (Abcam; Zotal, Tel-Aviv, Israel) were used (as indicated). The secondary antibodies were Texas Red (1:200, Jackson Immuno Research, PA, USA) or Dy light 649 (1:150 Jackson ImmunoResearch, Baltimore, USA). Mounting with Vectashield (Vector Laboratories, Burlingame, CA, USA).

Mice. The human PrP-A53T α-Syn tg mouse line(Giasson et al., 2002) was purchased from Jackson Laboratory (Bar Harbor, ME, USA) as hemizygous; cross-bred with C57BL/6JOlaHsd α-Syn$^{-/-}$ mice (Harlan Laboratories, Jerusalem, Israel (Specht and Schoepfer, 2001)) to silence endogenous mouse α-Syn; and then bred to achieve homozygosity of the human A53T α-Syn transgene. C57BL/6 wt mouse brains were used as control mice. All animal welfare and experimental protocols were approved by the Committee for the Ethics of Animal Experiments of the Hebrew University of Jerusalem NIH approval # OPRR-A01-5011 (Permit number: MD-16-14826-3).

Primary neuronal cultures.

Cortical neurons were prepared from C57BL/6 wt mouse brains as in (Ben Gedalya et al., 2009) with minor modifications. Briefly, hippocampal CA1-CA3 regions were dissected from 1 day-old C57BL/6 mouse brains, dissociated by trypsin treatment, followed by trituration with a siliconized Pasteur pipette and then plated onto coverslips coated with poly-D-lysine (Sigma-Aldrich, Rehovot, Israel) inside 24-well dish. Culture medium consisted of MEM (Invitrogen, Rhenium,

Israel), 0.6% glucose, 0.1 gm/L bovine Tf (Sigma-Aldrich), 0.25 gm/L insulin (Sigma-Aldrich), 0.3 gm/L glutamine, 5–10% fetal calf serum (Sigma- Aldrich) and 2% B-27 supplement (Invitrogen, Rhenium, Israel). To eliminate the glial cells, 8 mM cytosine b-D-arabinofuranoside (Sigma-Aldrich) was added to the culture 3 days after preparation and removed after additional 3–4 days. Cultures were maintained at 378C in a 95% air/5% CO2 humidified incubator, and culture medium was replaced every 4–7 days.

Mesencephalic neurons were prepared from brains of mice at E13.5 embryos as described (Zaltieri et al., 2015) with minor modifications. Briefly, ventral mesencephalic tissues were dissected from C57BL/6J and C57BL/6JOlaHsd mice at embryonic day 13.5. After mechanical dissociation, the single cell suspension was resuspended in Neurobasal medium (Biological Industries, Bet Haemek, Israel) containing 100 µg/ml penicillin, 100 µg/ml streptomycin (Sigma-Aldrich, Rehovot, Israel), 2 mM glutamine (Biological Industries) and 1% B27 supplement (Biological Industries); cells were then centrifuged. Cell count and viability assays were performed using the Trypan Blue exclusion test. Cells were seeded onto poly-D-Lysine-coated glass coverslides in 24-well plates for immunocytochemistry, or onto poly-D-Lysine coated Petri dishes for western blot or transmission electron microscopy analyses. Cells were maintained at 37°C under a humidified atmosphere of 5% CO_2 and 95% O_2 in Neurobasal medium for 10 days *in vitro*.

Electroporation of primary neurons was performed on day of preparation using Amaxa Nucleofecto (Lonza, Tuas, Singapore) according to manufacture's protocol (Vieira et al., 2016). 0.2- 1.0 × 10^6 cells were suspended in 100µl of Ingenio electroporation solution (Mirus Bio LLC, Madison, WI, USA) containing 2.5 µg of DNA, in a nucleofection cuvette using program O-05. Cells were then plated as above.

Images were acquired using a Zeiss LSM 710 Axio Observer confocal Z1 laser scanning microscope, equipped with an argon laser 488, Diode 405-430 laser and HeNe 633 laser. Per each experiment, exciting laser, intensity, background levels, photo multiplier tube (PMT) gain, contrast and electronic zoom were maintained constant. For each antibody, the background was subtracted (determined by a negative control consisting of the secondary antibody alone). The zoom of each picture was obtained by choosing the plane with greatest fluorescent signal.

Quantification of nuclear localization were performed blinded to treatments. To reduce experimental error, comparisons were made within slides that were processed and analysed in parallel. Image series were analyzed with Fiji (Image J, National Institutes of Health). For nuclear localization of α-Syn, the area of the nucleus was defined according to the signal obtained for DAPI. α-Syn signal that colocalized with the area stained with DAPI was defined as nuclear α-Syn signal and subtracted from whole cell α-Syn signal to obtain the cytosolic α-Syn. In each experiment a mean ± SD of minimum n=20 cells is presented.

Determination of luciferase activity. MCF7 cells were transfected to express the indicated DNA plasmids. Twenty four hours post transfection, the conditioning medium was replaced to contain the activating ligands, or their corresponding controls in 0.1% FBS-supplemented DMEM. For RA or other retinoids, cells were treated with 50 nM, or 0.05% DMSO. For fatty acid treatment, either one of the following fatty acids: OA (18:1), LA (18:2), ALA (18:3) or DHA (22:6), were pre-incubated with BSA in binding buffer containing 150 mM NaCl and 10 mM Tris-Cl pH 7.5 at 37°C, for 30 minutes and filtered through 48 micron filters. Cells were conditioned with a final concentration of 0.25 mM fatty acid/0.05 mM BSA. Control cells were treated with BSA only at 0.05 mM. At 48 hours post-transfection cells were harvested, washed twice in clean DMEM and lysed in a luciferase assay-buffer, containing 100 mM Tris-acetate pH 7.5, 10 mM magnesium acetate, 1 mM EDTA, 2 mM DTT, protease inhibitor cocktail (1X; Sigma Aldrich, Rehovot, Israel) and 1% Triton X-100, by incubation for 20 minutes on ice. The homogenate was centrifuged at 10,000 xg for 5 minutes. The supernatant was transferred to a clean tube. Each sample was tested in triplicate. Samples of 15 µl lysed cells were loaded on a white Greiner 96-wells plate (Sigma-Aldrich, Rehovot, Israel) and 100 µl of luciferase assay buffer, containing 10 mM luciferine (Sigma-Aldrich) and 100 mM ATP (Sigma-Aldrich) were added to each well, in triplicates. Luminescence was determined using Infinite M200 Pro plate-reader (Thermo Fisher, Qiryat Shemona, Israel).

β-galactosidase (β-gal) assay, sample (20 µl) were loaded on a Thermo-Fisher flat transparent 96-well plate in triplicates. Eighty µl β-gal buffer [50 mM KH_2PO_4, 1 mM $MgCl_2$, and 1 mM chlorophenol red-β-D-galactopyranoside (CPRG), pH 7.5] were added to each well. The plate was incubated for 10 minutes at 37°C and absorbance was measured using Infinite M200 Pro plate

reader (ThermoFisher, Petah Tiqva, Israel). Protein concentration was determined using Pierce BCA Protein Assay Kit (Thermo Fisher). Luciferase counts were normalized to protein concentration and β-gal activity for each test sample.

Isothermal titration calorimetry (ITC) data collection. All experiments were performed at 25 °C on high-feedback mode with a stirring speed of 750 r.p.m. (Malvern PEAQ-ITC). Purified α-Syn protein (10 μM in 150 mM NaCl, 10 mM Tris-cl pH 7.5) was added to the reaction cell and the ligand to the injection syringe. The concentration of RA in the injection syringe was 100 μM and the concentration of OA (18:1) or ALA (18:3) was 200 μM. The solutions were allowed to reach 25 °C for ~5 minutes prior to starting the experiment. Injections were monitored at a volume of 2 μl and in 180 seconds intervals. In reactions containing the organic DMSO solvent, both α-Syn protein and the ligand were brought to the same final DMSO concentration of 1%. A baseline correction procedure was implemented.

ImageStream Analysis. MCF7 cells were washed with clean DMEM and fixed in 2% paraformaldehyde for 10 minutes on ice. Cells were washed three times with DMEM and re-suspended in permeabilization buffer containing 0.1% Triton X-100 and 1% BSA in PBS for 5 minutes at room temperature. Cells were then incubated in blocking solution containing 1% BSA in PBS for 10 minutes and then incubated with a primary antibody, MJF-1 (1:250, Abcam. Zotal, Tel Aviv, Israel) for one hour at room temperature, washed 3 timed with DMEM and incubated with secondary antibody, Dy light 649 (1:150 Jackson ImmunoResearch, Baltimore, USA) for one hour at room temperature. Diamidino-2-phenylindole (DAPI; 1 mg/ml) was added to cells for 15 minutes before the end of the incubation with the secondary antibody. Cells were washed twice in clean DMEM and then analyzed.
Images were acquired on the ImageStream X MKII imaging cytometer (Amnis Corp, WA, USA). Data analysis was performed using Nuclear Localization Wizard, IDEAS® image analysis software package (Amnis Corp). 4000-6000 events were collected for each sample on an ImageStream IS100 using 649 nm laser excitation. Cell populations were sequentially gated for single cells that were singular, round, in focus and positive for both α-Syn and DAPI. Following application of gating, the acquired images were analyzed for intensity and saturation of signals. The spatial localization of α-Syn and DAPI was measured using the “Similarity” feature in the IDEAS®

software package. The “Similarity Score”, a log transformed Pearson's correlation coefficient between the pixel values of two image pairs, provided a measure of the degree of nuclear localization of α-Syn by measuring the pixel intensity correlation between the α-Syn immunoreactivity and DAPI images.

Lipid-ELISA was performed as previously described (Abd-Elhadi et al., 2016). Briefly, a 96-well PolySorp ELISA plate was coated with phospholipids and GM-1 ganglioside at a final amount of 5 µg/well. Wells were blocked with 100 µl of 1 % BSA (fatty acid-free) in PBS. Test samples were added into the wells, in triplicates and incubated overnight at 4 °C to allow capture of proteins by the immobilized lipids. The wells were washed with PBS (Ca^{2+} and Mg^{2+} free). Bound PSer129 α-Syn detection with monoclonal antibody (pSyn#64, WAKO, Osaka, Japan) diluted 1:1000 in 1% BSA in PBS. Following incubation for one hour at 37 ºC, the wells were washed 3 times and then incubated with a secondary antibody for one hour at 37 ºC (Jackson Laboratories, ENCO, Israel) diluted 1:8000 in 1% BSA in PBS and washed three times as above. Detection with Super Signal ELISA Femto (Pierce, Ornat, Israel) for the enzymatic reaction. Luminescence was determined by Luminometer (Infinite M200 Pro. NEOTEL Scientific Instrumentation Ltd.) immediately after adding the substrate. A standard curve consisting of recombinant protein, phosphorylated at Ser129 (Proteos, Kalamazoo, US), was applied in parallel to test samples and used as a reference.

Statistical analyses

Comparisons between two groups were performed by two tailed T test. Additional comparisons were performed by one way ANOVA. Data presented as mean ± SD or mean ± SE, as indicated. Significant differences were considered with $P< 0.05$.

Supplemental Table 1. PCR primers

Gene	Forward (5→3)	Reverse (5→3)
m. α-Syn	CATCTTTAGCCATGGATGTG	CCCATCTGGTCCTTCTTGAC
m. CRABP2	GATCCTGACAATGACAGCAGATG	TCGTCTCAGGCAGTTCTTGGA
m. RBP1	GCGCTCGACGTCAACGT	TCAGCGTGCGGATGATCAT
m. CRABP1	CGCCGCTACAGCCAACAC	TTCACACCCAACGCCTTGA
m. RBP4	TCCAGCGAGGAAACGATGAC	GCACAGGTGCCATCCAGATT
m. 18S	5-GCCAGAACCTGGCTGTACTT	5-GAGCGAGTGATCACCATCAT
h. DDC	AAGTCGGTCCTATCTGCAACAAG	TTCAGAAGGTGCCGGAACTC
h. PINK1	TATGGAGCAGTCACTTACAGAAAA TCC	GGTGAAGGCGCGGAGAA
h. ADORA1	CATCCCTCTGGAGCTTACCG	CAAGCACCCAAGGTCACCAA
h. FTL	CCATGAGCTCCCAGATTCGT	GGTCGAAATAGAAGCCCAGAGA
h. ATP13A2	ATGATGGCTGGGATCCCTTT	AACTATCCTCTTTGTCTCTTATTTCGAT AAC
h. α-Syn	GCAGGGAGCATTGCAGCAGC	GGCTTCAGGTTCGTAGTCTTG
h.CRABP2	AAAATGGTCTGTGAGCAGAAGCT	CCGTCATGGTCAGGATCAGTT
h. RBP1	CGCCCTCGACGTCAATGT	CAGCGTGCGGATGATCATAT
h. CRABP1	TCCACTGCACGCAAACTCTT	CAAACGTCAGGATAAGTTCATCGT
h. RBP4	TGATCGTCCACAACGGTTACTG	AGCTGAAGACTGAGAGCTAATCAGAA
h. PIN1	GCAGCTCAGGCCGAGTGTA	CCCGTTTTTGCCACCACTG
h. STUB1	GGCCAAGCACGACAAGTACA	CAAAGCTGATCTTGCCACACA
h. RARa	GGCCTGTTTGCTCCCAGAGAA	GAGGGCTGGGCACTATCTCTT
h. RARb	ACAGCTGAGTTGGACGATCTCA	CACTGGAATTCGTGGTGTATTTACC
h. RET	GGCCGAGATGAAGCTCGTT	CAAGCCGAAATCCGAAATCTT
h. G6PD	5-CACCATCTGGTGGCTGTTC	5-TCACTCTGTTTGCGGATGTC
WPRE	CCGTTGTCAGGCAACGTG	AGCTGACAGGTGGTGGCAAT

m, mouse; h, human

Supplemental References

ABD-ELHADI, S., BASORA, M., VILAS, D., TOLOSA, E. & SHARON, R. 2016. Total alpha-synuclein levels in human blood cells, CSF, and saliva determined by a lipid-ELISA. *Anal Bioanal Chem,* 408**,** 7669-7677.

ASSAYAG, K., YAKUNIN, E., LOEB, V., SELKOE, D. J. & SHARON, R. 2007. Polyunsaturated Fatty Acids Induce alpha-Synuclein-Related Pathogenic Changes in Neuronal Cells. *Am J Pathol,* 171**,** 2000-11.

BEN GEDALYA, T., LOEB, V., ISRAELI, E., ALTSCHULER, Y., SELKOE, D. J. & SHARON, R. 2009. Alpha-synuclein and polyunsaturated fatty acids promote clathrin-mediated endocytosis and synaptic vesicle recycling. *Traffic,* 10**,** 218-34.

FANNING, S., HAQUE, A., IMBERDIS, T., BARU, V., BARRASA, M. I., NUBER, S., TERMINE, D., RAMALINGAM, N., HO, G. P. H., NOBLE, T., SANDOE, J., LOU, Y., LANDGRAF, D., FREYZON, Y., NEWBY, G., SOLDNER, F., TERRY-KANTOR, E., KIM, T. E., HOFBAUER, H. F., BECUWE, M., JAENISCH, R., PINCUS, D., CLISH, C. B., WALTHER, T. C., FARESE, R. V., JR., SRINIVASAN, S., WELTE, M. A., KOHLWEIN, S. D., DETTMER, U., LINDQUIST, S. & SELKOE, D. 2018. Lipidomic Analysis of alpha-Synuclein Neurotoxicity Identifies Stearoyl CoA Desaturase as a Target for Parkinson Treatment. *Mol Cell*.

GIASSON, B. I., DUDA, J. E., QUINN, S. M., ZHANG, B., TROJANOWSKI, J. Q. & LEE, V. M. 2002. Neuronal alpha-synucleinopathy with severe movement disorder in mice expressing A53T human alpha-synuclein. *Neuron,* 34**,** 521-33.

GOLOVKO, M. Y., BARCELO-COBLIJN, G., CASTAGNET, P. I., AUSTIN, S., COMBS, C. K. & MURPHY, E. J. 2009. The role of alpha-synuclein in brain lipid metabolism: a downstream impact on brain inflammatory response. *Mol Cell Biochem,* 326**,** 55-66.

HOFFMAN, L. M., GARCHA, K., KARAMBOULAS, K., COWAN, M. F., DRYSDALE, L. M., HORTON, W. A. & UNDERHILL, T. M. 2006. BMP action in skeletogenesis involves attenuation of retinoid signaling. *J Cell Biol,* 174**,** 101-13.

LOVE, M. I., HUBER, W. & ANDERS, S. 2014. Moderated estimation of fold change and dispersion for RNA-seq data with DESeq2. *Genome Biol,* 15**,** 550.

SHARON, R., BAR-JOSEPH, I., FROSCH, M. P., WALSH, D. M., HAMILTON, J. A. & SELKOE, D. J. 2003a. The formation of highly soluble oligomers of alpha-synuclein is regulated by fatty acids and enhanced in Parkinson's disease. *Neuron,* 37**,** 583-95.

SHARON, R., BAR-JOSEPH, I., MIRICK, G. E., SERHAN, C. N. & SELKOE, D. J. 2003b. Altered fatty acid composition of dopaminergic neurons expressing alpha-synuclein and human brains with alpha-synucleinopathies. *J Biol Chem,* 278**,** 49874-81.

SHARON, R., GOLDBERG, M. S., BAR-JOSEF, I., BETENSKY, R. A., SHEN, J. & SELKOE, D. J. 2001. alpha-Synuclein occurs in lipid-rich high molecular weight complexes, binds fatty acids, and shows homology to the fatty acid-binding proteins. *Proc Natl Acad Sci U S A,* 98**,** 9110-5.

SLADEK, F. M., ZHONG, W. M., LAI, E. & DARNELL, J. E., JR. 1990. Liver-enriched transcription factor HNF-4 is a novel member of the steroid hormone receptor superfamily. *Genes Dev,* 4**,** 2353-65.

SPECHT, C. G. & SCHOEPFER, R. 2001. Deletion of the alpha-synuclein locus in a subpopulation of C57BL/6J inbred mice. *BMC Neurosci,* 2**,** 11.

VARGA, T., CZIMMERER, Z. & NAGY, L. 2011. PPARs are a unique set of fatty acid regulated transcription factors controlling both lipid metabolism and inflammation. *Biochim Biophys Acta,* 1812**,** 1007-22.

VIEIRA, M. M., SCHMIDT, J., FERREIRA, J. S., SHE, K., OKU, S., MELE, M., SANTOS, A. E., DUARTE, C. B., CRAIG, A. M. & CARVALHO, A. L. 2016. Multiple domains in the C-terminus of NMDA receptor GluN2B subunit contribute to neuronal death following in vitro ischemia. *Neurobiol Dis,* 89**,** 223-34.

WISELY, G. B., MILLER, A. B., DAVIS, R. G., THORNQUEST, A. D., JR., JOHNSON, R., SPITZER, T., SEFLER, A., SHEARER, B., MOORE, J. T., MILLER, A. B., WILLSON, T. M.

& WILLIAMS, S. P. 2002. Hepatocyte nuclear factor 4 is a transcription factor that constitutively binds fatty acids. *Structure,* 10**,** 1225-34.
ZALTIERI, M., GRIGOLETTO, J., LONGHENA, F., NAVARRIA, L., FAVERO, G., CASTREZZATI, S., COLIVICCHI, M. A., DELLA CORTE, L., REZZANI, R., PIZZI, M., BENFENATI, F., SPILLANTINI, M. G., MISSALE, C., SPANO, P. & BELLUCCI, A. 2015. alpha-synuclein and synapsin III cooperatively regulate synaptic function in dopamine neurons. *J Cell Sci,* 128**,** 2231-43.